Surface and size dependent effects on static, buckling, and vibration of micro composite beam under thermo-magnetic fields based on strain gradient theory

Mehdi Mohammadimehr [*1], Mojtaba Mehrabi [1], Hasan Hadizadeh [1,2] and Hossein Hadizadeh [1,2]

[1] *Department of Solid Mechanics, Faculty of Mechanical Engineering, University of Kashan, P.O. Box 87317-53153, Kashan, Iran*
[2] *Department of Solid Mechanics, Faculty of Mechanical Engineering, University of Tehran, Tehran, Iran*

Abstract. In this article, static, buckling and free vibration analyses of a sinusoidal micro composite beam reinforced by single-walled carbon nanotubes (SWCNTs) with considering temperature-dependent material properties embedded in an elastic medium in the presence of magnetic field under transverse uniform load are presented. This system is used at micro or sub micro scales to enhance the stiffness of micro composite structures such as bar, beam, plate and shell. In the present work, the size dependent effects based on surface stress effect and modified strain gradient theory (MSGT) are considered. The generalized rule of mixture is employed to predict temperature-dependent mechanical and thermal properties of micro composite beam. Then, the governing equations of motions are derived using Hamilton's principle and energy method. Numerical results are presented to investigate the influences of material length scale parameters, elastic foundation, composite fiber angle, magnetic intensity, temperature changes and carbon nanotubes volume fraction on the bending, buckling and free vibration behaviors of micro composite beam. There is a good agreement between the obtained results by this research and the literature results. The obtained results of this study demonstrate that the magnetic intensity, temperature changes, and two parameters elastic foundations have important effects on micro composite stiffness, while the magnetic field has greater effects on the bending, buckling and free vibration responses of micro composite beams. Moreover, it is shown that the effects of surface layers are important, and observed that the changes of carbon nanotubes volume fraction, beam length-to-thickness ratio and material length scale parameter have noticeable effects on the maximum deflection, critical buckling load and natural frequencies of micro composite beams.

Keywords: static; buckling; vibration; micro composite beam; surface effect; magnetic and thermal fields

1. Introduction

In the last decades, due to carbon nanotubes (CNTs) extremely mechanical, magnetic and thermal properties the use of them is attracted a great deal of interest of researchers. They have many applications in polymer composites as reinforcement. Thus, nowadays, these materials are used as reinforcement in micro or sub micro scales to enhance the stiffness of micro composite structures such as bar, beam, plate and shell. It is reported in some experimental studies that the structures become stiffer in smaller scales such as Poole *et al.* (1996), Lam *et al.* (2003) and McFarland and Colton (2005). Moreover, these materials are used in nanotechnology because of the intensive reduces in grain sizes of nanocrystalline materials (NcMs), a large volume fraction of atoms reside in the interface regions between crystals forming anatom-cloud phase with a distinct atomic structure (Shaat 2015). Moreover, the surface to volume ratio of the grain increases. Thus, its surface energy will significantly affect the mechanical properties of NcMs (Shaat 2015). There are many mathematical and physical theories in order to simulate the effect of micro/ nano scale in various structures, but classical continuum theories do not predict the microstructure-dependent deformation behavior of micro and Nano-sized structures (Aifantis 1999). Thus, to consider the size dependent effect, the researchers are employed several non-classical continuum theories such as micropolar (Eringen 1967) and nonlocal elasticity (Eringen 1972), surface stress effect, and strain gradient (Fleck and Hutchinson 1993, 2001) and couple stress theories (Koiter 1964). Some researchers investigated bending, buckling and free vibration analysis of various structures based on size dependent effects at micro or nano scales. Shaat and Abdelkefi (2015) considred influences of the nano crystalline silicon (Nc–Si) material structure on the pull-in instability of nanobeams subjected to a distributed electrostatic force. They presented a size-dependent micromechanical and atomic lattice models for multi-phase materials considering the in homogeneities surface energy effects and in order to investigate elastic modulus of the interface of NcMs, respectively. Also, in the other study (Shaat and Abdelkefi 2017), they discussed about effects of the grain size, the voids percent and size, and the grain boundary (interface) of nonlinear model for electrostatically actuated nanocrystalline beams accounting for the beam

---

∗Corresponding author, Ph.D., Associate Professor,
  E-mail: mmohammadimehr@kashanu.ac.ir

material structure. Akgöz and Civalek (2015a) investigated bending response of non-homogenous microbeams embedded in an elastic foundation based on modified strain gradient elasticity theory (MSGT) in conjunctions with Euler-Bernoulli, Timoshenko, Parabolic (third-order) beam, and sinusoidal (trigonometric) beam theories. Simsek and Reddy (2013) studied influences of the material length scale parameter, different material composition, and shear deformation on the bending and free vibration behaviors of functionally graded (FG) microbeams based on modified couple stress theory (MCST). Mohammadimehr and Mehrabi (2017) developed stability and free vibration analyses of double-bonded micro composite sandwich cylindrical shells conveying fluid flow under magneto-thermo-mechanical loadings based on the MCST and third order shear deformation cylindrical shells theory (TSDT). They investigated that the effect of static fluid flow in the both of cylindrical shells in comparison with influences of flow in the one of them is the same for the moderately thick-walled micro cylindrical shells. The effects of power-low index of material gradient, plate aspect ratio and mechanical and electric loadings on the displacement and natural frequency of FG piezoelectric micro plate based on MCST are demonstrated by Li and Pan (2015). Ghorbanpour Arani and Roudbari (2014) considered the electro-thermal nonlocal wave propagation of fluid-conveying single-walled boron nitride nanotubes (SWBNNTs) using nonlocal piezo-elasticity with surface stress, initial stress and Knudsen-dependent flow velocity effect. They showed that the results of their article can be used in design and manufacturing of smart micro electro mechanical systems (MEMS) and nano electro mechanical systems (NEMS) in advanced medical application such as drug delivery systems with great application in biomechanics. Ansari *et al*. (2011) showed that the value of gradient index plays an important role in the vibrational response of the FG Timoshenko micro beams. Lei *et al*. (2013b) studied the buckling analysis of functionally graded carbon nanotube reinforced composite (FG-CNTRC) plates under various in-plane mechanical loads, using the element-free-*kp*-Ritz method. Their results demonstrated that the change of carbon nanotube volume fraction, loading condition and temperature have especial effect on buckling strength of CNTRC plates. Akgöz and Civalek (2014a) illustrated a new microstructure-dependent sinusoidal beam model for buckling of micro beams that the size dependency becomes more important when the thickness of the micro beam is closer to material length scale parameter. Mohammadimehr *et al*. (2016b) investigated bending, buckling and free vibration behaviors of micro composite plate reinforced by FG-SWCNT under hydro-thermal environments using TSDT and MSGT. They are shown that with increasing of moisture change reduces the natural frequency and critical buckling load and increases the deflection of micro composite plate. Civalek *et al*. (2009) studied static analysis of CNT using nonlocal Euler-Bernoulli beam theory (EBT). They used differential quadrature method (DQM) for bending analysis of numerical solution of CNTs. Afshin and Taheri (2015) discussed about static bending analysis of the interlaminar

stresses and free edges effect in a laminated composite beam resting on the Winkler-type elastic foundation and demonstrated that the magnitude of interlaminar stresses are significant and should be considered in the structural design. Ma *et al*. (2008) considered the static and free vibration problems of MCST and classical Timoshenko beams that both the deflection and rotation of the simply supported beam predicted by the MCST are smaller than those predicted by the classical Timoshenko beam. Thai and Vo (2013a) used from a new sinusoidal shear deformation theory for bending, buckling and vibration analyses of FG plates and concluded that this theory is accurate and efficient in predicting the bending, buckling and vibration responses of FG plates. Lei *et al*. (2013a) introduced a novel size-dependent beam model made of FGM based on MSGT and established that the FG micro beams exhibit significant size-dependent when the thickness of the micro beam approach to the material length scale parameter. Jahangiri *et al*. (2015) investigated nonlinear mechanical behavior of the FGM micro-gripper under thermal load and DC voltage taking into account the effect of intermolecular forces based on MCST using the Galerkin based step-by-step linearization method (SSLM). Yang *et al*. (2014) investigated the vibration and damping characteristics of free-free composite sandwich cylindrical shell with pyramidal truss-like cores using the Rayleigh-Ritz model and finite element method (FEM). Also, their predictions for the modal properties of composite sandwich cylindrical shell with pyramidal truss-like cores showed good agreement with the experimental tests. Dai *et al*. (2016) predicted the nonlinear forced vibration behavior of a cantilever nanobeam, essentially considering the surface elastic layer. The results of their research demonstrated that the combined effects of the residual stress and aspect ratio on the maximum amplitude of the nanobeam may be pronounced. Zhu *et al*. (2012) examined the effects of carbon nanotubes volume fraction, plate width-to-thickness (aspect) ratio, plate side ratio, boundary conditions, load type and distribution type of CNTs on the dynamic responses of CNTR-FG plates using the element-free-*KP*-Ritz method and finite element method (FEM) based on first order shear deformation theory (FSDT). Shen (2009) investigated the nonlinear bending of FG nanocomposite plates reinforced by SWCNTs subjected to a transverse uniform or sinusoidal load in thermal environments. Their results showed that the load-bending moment curves of the plate can be significantly increased as a result of FG reinforcement. Ansari and Sahmani (2011) considered the effects of surface stresses on free vibration behavior of classical (CLPT) and FSDT nanoplate and found that the difference between the results predicted by the classical and non-classical solutions relies on the sign and magnitude of the surface elastic constants.

The study of the researches indicates that there is not any work about static, buckling and free vibration analyses of a sinusoidal micro composite beam reinforced by SW-CNTs with considering temperature-dependent material properties embedded in an elastic medium in presence of magnetic field under axial and transverse uniform loads is presented. In this work, the size dependent effects based on

the surface stress effect and MSGT are considered simultaneously. The generalized rule of mixture is employed to predict temperature-dependent mechanical and thermal properties of micro composite beam. Then, the governing equations of motions are derived using Hamilton's principle. Numerical results are presented to investigate the influence the material length scale parameters, elastic foundation, composite fiber angle, magnetic intensity, temperature changes and CNTs volume fraction on the bending, buckling and free vibration behavior of micro beam. It is noted that in this study, the effects of fiber angle and intensity of magnetic field are considered as well as temperature change on the dimensionless natural frequencies, critical buckling load and maximum deflection of micro composite beam that there is not in the previous researches. Also, it can be seen that the considering of the surface stress effect on the behaviors of micro sinusoidal beams is the other novelty of this article.

2. Geometry of sinusoidal micro composite beam reinforced by CNTs

According to Fig. 1(a), the micro composite sinusoidal beam reinforced by CNTs in presence of magnetic fields considered with length L, width b and thickness h.

This micro composite beam rested on elastic foundation with Winkler spring coefficient k_w and Pasternak shear modulus k_G. Uniformly distribution (UD) of single-walled carbon nanotubes (UD-SWCNTs) in micro beam are considered that is shown in Fig. 1(b). Carbon nanotubes volume fraction for this distribution is defined as follows (Mohammadimehr *et al.* 2016b, Lei *et al.* 2013a)

$$V_{CNT}(z) = V_{CNT}^{*} \tag{1a}$$

where

$$V_{CNT}^{*} = \frac{w_{CNT}}{w_{CNT} + (\frac{\rho_{CNT}}{\rho_m})(1 - w_{CNT})} \tag{1b}$$

where w_{CNT}, ρ_m and ρ_{CNT} are SWCNTs mass fraction, matrix density and SWCNTs density, respectively.

3. Extended mixture rule

According to the extended mixture rule, effective material properties of micro composite sinusoidal beams can be expressed as follows (Ansari and Sahmani 2011)

$$E_{11} = \eta_1 V_{CNT} E_{11}^{CNT} + V_m E_m \tag{2a}$$

$$\frac{\eta_2}{E_{22}} = \frac{V_{CNT}}{E_{22}^{CNT}} + \frac{V_m}{E_m} \tag{2b}$$

$$\frac{\eta_3}{G_{12}} = \frac{V_{CNT}}{G_{12}^{CNT}} + \frac{V_m}{G_m} \tag{2c}$$

$$\rho = V_{CNT}\rho_{CNT} + V_m\rho_m \tag{2d}$$

$$\upsilon_{12} = V_{CNT}\upsilon_{12}^{CNT} + V_m\upsilon_m \tag{2e}$$

$$\alpha_{11} = V_{CNT}\alpha_{11}^{CNT} + V_m\alpha^m \tag{2f}$$

where E_{11}^{CNT} and E_{22}^{CNT} are Young's modulus of SWCNTs in longitudinal and transverse directions, respectively. G_{12}^{CNT} is the shear modulus of SWCNTs. E_m and G_m denote Young's modulus and shear modulus of the isotropic matrix. Also η_i ($i = 1, 2, 3$) denotes force transformation between
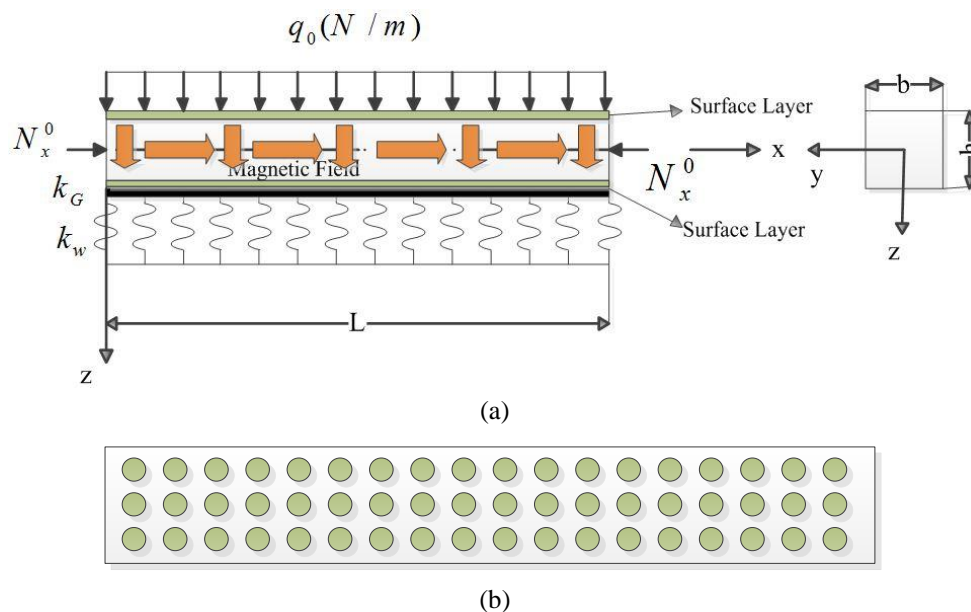

Fig. 1 (a) Geometry of micro composite sinusoidal beam in an elastic foundation in the presence of magnetic field; (b) distribution of SWCNTs in micro composite sinusoidal beam

Table 1 η_i coefficient of SWCNTs (Mohammadimehr *et al.* 2016b)

0.11	0.149	0.934	0.934
0.14	0.150	0.941	0.941
0.17	0.149	1.381	1.381

SWCNTs and polymeric matrix. It is defined the extended mixture rule as the following form

$$V_m + V_{CNT} = 1 \tag{3}$$

where V_m is the matrix volume fraction.

The temperature-dependent mechanical properties of PmPv as the matrix are considered as follows (Lei *et al.* 2013c, Mohammadimehr *et al.* 2016b)

$$\upsilon_m = 0.34 \tag{4a}$$

$$\alpha_m = 45(1 + 0.0005\Delta T) \times 10^{-6} / K \tag{4b}$$

$$E_m = (3.51 - 0.0047T) GPa \tag{4c}$$

where $\Delta T = T - T_0$ and $T_0 = 300\ K$. It is noted that the temperature of the top and bottom surfaces is the same.

The temperature-dependent material properties of SWCNTs as reinforcement are obtained as quadratic curve using Lagrange polynomials from data in Lei *et al.* (2015)

$$E_{11}^{CNT} = (7.425 \times 10^5 T^2) - (1.173 \times 10^9 T) + (5.9317 \times 10^{12}) \tag{5a}$$

$$E_{22}^{CNT} = (9.3125 \times 10^5 T^2) - (1.471 \times 10^9 T) + (7.4375 \times 10^{12}) \tag{5b}$$

$$G_{12}^{CNT} = (-2.4625 \times 10^5 T^2) + (2.96 \times 10^8 T) + (1.8779 \times 10^{12}) \tag{5c}$$

$$\rho^{CNT} = 4000(Kg / m^3) \tag{5d}$$

$$\alpha_{11}^{CNT} = (-1.1826 \times 10^{-11} T^2) \cdot$$
$$+ (1.4850 \times 10^{-8} T) + (6.7913 \times 10^{-8}) \tag{5e}$$

Finally, η_i coefficient for different SWCNTs volume fractions are shown in Table 1 (Zhu *et al.* 2012).

4. Formulation

4.1 Displacement equations

Formulation of bending, buckling and free vibration of micro composite beams is derived using Hamilton's principle. The displacement fields based on the sinusoidal shear deformation theory (SSDT) can be expressed as follows (Akgöz and Civalek 2014a).

$$u(x,z,t) = u_0(x,t) - z\frac{\partial w_0(x,t)}{\partial x} + R(z)\Phi_X(x,t) \tag{6a}$$

$$v(x,z,t) = 0 \tag{6b}$$

$$w(x,z,t) = w_0(x,t) \tag{6c}$$

In which

$$R(z) = \frac{h}{\pi}\sin(\frac{\pi}{h}z) \tag{6d}$$

where u, v and w are the displacements of micro beam in x, y and z direction, respectively, and ϕ_x is the angle of rotation of the cross-section of any point on the mid-plane of the beam. $R(z)$ is a function of z and plays a role in calculation of the transverse shear strain and stress distribution throughout the height of the beam.

4.2 The modified strain gradient theory

One of the non-classical theories is the modified strain gradient theory (MSGT) (Akgöz and Civalek 2015a), in which, there are higher-order deformation gradients. According to this theory, the first variation of strain energy U can be written with infinitesimal deformations as (Akgöz and Civalek, 2014b, 2015a, 2016)

$$\delta U = b\int_0^L \int_{-\frac{h}{2}}^{\frac{h}{2}} (\sigma_{ij}\delta\varepsilon_{ij} + p_i\delta\gamma_i + \tau_{ijk}^{(1)}\delta\eta_{ijk}^{(1)} + m_{ij}^{(s)}\delta\chi_{ij}^{(s)})dzdx \tag{7}$$

where σ_{ij}, p_i, $\tau_{ijk}^{(1)}$, $m_{ij}^{(s)}$ are the components of classical σ and higher-order stress tensor P, $\tau^{(1)}$, $m_i^{(s)}$ can be described as follows (Mohammadimehr *et al.* 2016a, Attia and Mahmud 2016)

$$\begin{Bmatrix} \sigma_X \\ \tau_{xz} \end{Bmatrix} = \begin{bmatrix} C_{11} & 0 \\ 0 & C_{55} \end{bmatrix} \begin{Bmatrix} \varepsilon_X - \alpha_{11}\Delta T \\ \gamma_{xz} \end{Bmatrix} \tag{8a}$$

$$P_i = 2Gl_0^2\gamma_i \tag{8b}$$

$$\tau_{ijk}^{(1)} = 2Gl_1^2\eta_{ijk}^{(1)} \tag{8c}$$

$$m_{ij}^{(s)} = 2Gl_2^2\chi_{ij} \tag{8d}$$

where in Eq. (8a), α_{11} is thermal expansion coefficients that is defined in Eq. (2), ΔT, is temperature changes and C_{11} is the transformation reduced plane stiffness, C_{55} is the transformation transverse shear stiffness and they can be defined as (Yang *et al.* 2014)

$$C_{11} = Q_{11}cos^4\theta + 2(Q_{12} + 2Q_{66})sin^2\theta cos^2\theta + Q_{22}sin^4\theta \tag{9a}$$

$$C_{55} = Q_{55} \tag{9b}$$

where θ is the composite fiber angle and $[Q_{ij}](i, j = 1, 2, 5, 6)$ are the local fiber-adapted coordinate reduced stiffness coefficients and can be describe as (Lei *et al.* 2013a)

$$Q_{11} = \frac{E_{11}}{1 - \upsilon_{12}\upsilon_{21}} \tag{10a}$$

$$Q_{22} = \frac{E_{22}}{1 - \upsilon_{12}\upsilon_{21}} \qquad (10b)$$

$$Q_{12} = \frac{\upsilon_{21}E_{11}}{1 - \upsilon_{12}\upsilon_{21}} \qquad (10c)$$

$$Q_{55} = G_{13} \qquad (10d)$$

In addition l_0, l_1 and l_2 are additional material length scale parameters related to dilatation, deviatoric stretch and rotation gradients, respectively. Also, the components of the classical strain tensor ε, the dilatation gradient vector γ, the deviatoric stretch gradient tensor $\eta^{(1)}$ and the symmetric rotation gradient tensor $\chi^{(s)}$ are defined as follows (Lei *et al.* 2013a, Mohammadi and Mahzoon 2013, Akgöz and Civalek 2015b)

$$\varepsilon_{ij} = \frac{1}{2}(u_{i,j} + u_{j,i}) \qquad (11a)$$

$$\gamma_i = \varepsilon_{mm,i} - \alpha_{ii}\Delta T \qquad (11b)$$

$$\eta_{ijk}^{(1)} = \frac{1}{3}(\varepsilon_{jk,i} + \varepsilon_{ki,j} + \varepsilon_{ij,k} - \alpha_{11}\Delta T) \\ - \frac{1}{15}\delta_{ij}(\varepsilon_{mm,k} + 2\varepsilon_{mj,m}) \\ - \frac{1}{15}\delta_{jk}(\varepsilon_{mm,i} + 2\varepsilon_{mi,m}) - \frac{1}{15}\delta_{ki}(\varepsilon_{mm,j} + 2\varepsilon_{mj,m}) \qquad (11c)$$

$$\chi_{ij}^{(s)} = \frac{1}{2}(e_{ipq}\varepsilon_{qj,x_p} + e_{jpq}\varepsilon_{qi,x_p}) \qquad (11d)$$

where u_i are the components of displacement field in x and z directions, e_{ipq} is the alternate tensor ($e_{123} = e_{231} = e_{312} = 1$, $e_{321} = e_{132} = e_{213} = -1$) and δ_{ij} is the Kronecker delta. It is noticeable that these equations are derived in Appendix A. By using Eqs. (11a)-(11d) and substituting them into Eqs. (8a)-(8d) and finally substituting these equations into Eq. (7), the first variation of strain energy U is defined as

$$\delta U = b\int_0^L \left\{ \begin{bmatrix} -N_{x,x} + P_{x,xx}^{(0)} + T_{xxx,xx}^{(0)} - T_{xyy,xx}^{(0)} - T_{xzz,xx}^{(0)} \end{bmatrix}\delta u_0 \\ + \begin{bmatrix} -M_{x,xx}^{(0)} + P_{x,xxx}^{(1)} - P_{z,xx}^{(0)} + T_{xxx,xxx}^{(1)} - T_{xzz,xx}^{(0)} - T_{xyy,xxx}^{(1)} - T_{xzz,xxx}^{(1)} + T_{yyz,xx}^{(0)} \\ + T_{zzz,xx}^{(0)} - M_{xy,xx}^{(0)} \end{bmatrix}\delta w_0 \\ + \begin{bmatrix} Q_{xz} - M_{x,x}^{(1)} + P_{x,xx}^{(2)} - P_{z,x}^{(0)} + T_{xxx,xx}^{(2)} - T_{xzz,x}^{(3)} - T_{xyy,x}^{(2)} - T_{xzz,xx}^{(3)} - T_{xzz,x}^{(2)} \\ + T_{xzz}^{(3)} + T_{yyz,x}^{(1)} + T_{zzz,x}^{(1)} - M_{xy,x}^{(1)} + M_{yz}^{(0)} \end{bmatrix}\delta\phi \right\} dx \qquad (12)$$

where

$$(N_x, M_x^{(0)}, M_x^{(1)}) = \int_{-\frac{h}{2}}^{\frac{h}{2}} \sigma_x(1, z, R)dz \qquad (13)$$

$$Q_{xz} = k_s \int_{-\frac{h}{2}}^{\frac{h}{2}} \sigma_{xz}\frac{\partial R}{\partial z}dz \qquad (14)$$

$$(P_x^{(0)}, P_x^{(1)}, P_x^{(2)}) = \int_{-\frac{h}{2}}^{\frac{h}{2}} p_x(1, z, R)dz \qquad (15a)$$

$$(P_z^{(0)}, P_z^{(1)}) = \int_{-\frac{h}{2}}^{\frac{h}{2}} p_z(1, \frac{\partial R}{\partial z})dz \qquad (15b)$$

$$(T_{xxx}^{(0)}, T_{xxx}^{(1)}, T_{xxx}^{(2)}, T_{xxx}^{(3)}) = \int_{-\frac{h}{2}}^{\frac{h}{2}} \frac{2}{5}\tau_{xxx}(1, z, R, \frac{\partial^2 R}{\partial z^2})dz \qquad (16a)$$

$$(T_{xzz}^{(0)}, T_{xzz}^{(1)}, T_{xzz}^{(2)}, T_{xzz}^{(3)}) = \int_{-\frac{h}{2}}^{\frac{h}{2}} \frac{3}{5}\tau_{xzz}(1, z, R, \frac{\partial^2 R}{\partial z^2})dz \qquad (16b)$$

$$(T_{xyy}^{(0)}, T_{xyy}^{(1)}, T_{xyy}^{(2)}, T_{xyy}^{(3)}) = \int_{-\frac{h}{2}}^{\frac{h}{2}} \frac{3}{5}\tau_{xyy}(1, z, R, \frac{\partial^2 R}{\partial z^2})dz \qquad (16c)$$

$$(T_{xxz}^{(0)}, T_{xxz}^{(1)}) = \int_{-\frac{h}{2}}^{\frac{h}{2}} \frac{4}{5}\tau_{xxz}(1, 2\frac{\partial R}{\partial z})dz \qquad (16d)$$

$$(T_{yyz}^{(0)}, T_{yyz}^{(1)}) = \int_{-\frac{h}{2}}^{\frac{h}{2}} \frac{1}{5}\tau_{yyz}(1, 2\frac{\partial R}{\partial z})dz \qquad (16e)$$

$$(T_{zzz}^{(0)}, T_{zzz}^{(1)}) = \int_{-\frac{h}{2}}^{\frac{h}{2}} \frac{1}{5}\tau_{zzz}(1, 2\frac{\partial R}{\partial z})dz \qquad (16f)$$

$$(M_{xy}^{(0)}, M_{xy}^{(1)}) = \int_{-\frac{h}{2}}^{\frac{h}{2}} m_{xy}(1, \frac{\partial R}{2\partial z})dz \qquad (17a)$$

$$M_{yz}^{(0)} = \int_{-\frac{h}{2}}^{\frac{h}{2}} \frac{1}{2}m_{yz}\frac{\partial^2 R}{\partial z^2}dz \qquad (17b)$$

4.3 The variation of surface stress effect

The classical ideas of continuum mechanics do not have the ability to apply the atomic features of the nano-structures. In this article, the modified continuum elasticity based on Gurtin-Murdoch theory is considered to develop analytical solutions for bending, buckling and free vibration of the micro composite beams reinforced by CNTs. The resulting in-plane loads lead to surface stresses which can be calculated using surface constitutive equations as (Ansari and Sahmani 2011, Lu *et al.* 2009a, b)

$$\sigma_x^s = (2\mu^s + \lambda^s)\varepsilon_x + \tau^s \qquad (18a)$$

$$\sigma_{xz}^s = \tau^s\frac{\partial w}{\partial x} \qquad (18b)$$

In which $2\mu + \lambda^s$ can defined as surface Lame constant (Ansari and Sahmani 2011)

$$E^s = 2\mu^s + \lambda^s \qquad (19)$$

where τ^s and E^s are the residual stress and surface Lame constants, respectively.

In the classical theories assumed that $\sigma_z = 0$, because the stress component σ_z is small in comparison with the

components of stress. Thus, it is unreal that omitted the σ_z and does not satisfy the surface conditions considered in the Gurtin-Murdoch model. So, it is assumed that σ_z varies through the beam thickness and satisfies the balance conditions on the upper and lower surfaces. On this assumption, σ_z can be calculated as (Ansari and Sahmani 2011, Shaat *et al.* 2012)

$$\sigma_z = \frac{(\frac{\partial \sigma_{xz}^s}{\partial x} - \rho^s \frac{\partial^2 w_0}{\partial t^2})_{TOP} - (\frac{\partial \sigma_{xz}^s}{\partial x} - \rho^s \frac{\partial^2 w_0}{\partial t^2})_{BOTTOM}}{2}$$
$$+ z \frac{(\frac{\partial \sigma_{xz}^s}{\partial x} - \rho^s \frac{\partial^2 w_0}{\partial t^2})_{TOP} - (\frac{\partial \sigma_{xz}^s}{\partial x} - \rho^s \frac{\partial^2 w_0}{\partial t^2})_{BOTTOM}}{h} \quad (20)$$

by using Eqs. (18) and (20), the stress component σ_z is defined as

$$\sigma_z = \frac{2z}{h}(\tau^s \frac{\partial^2 w_0}{\partial x^2} - \rho^s \frac{\partial^2 w_0}{\partial t^2}) \quad (21)$$

also, the first variation of surface energy can be written as (Mohammadimehr *et al.* 2014)

$$\delta U^s = \int_A (\sigma_x^s \delta \varepsilon_x + \sigma_{xz}^s \delta \varepsilon_{xz}) dA \quad (22)$$

Substituting Eq. (18) into Eq. (22), the variation of surface energy is defined as

$$\delta U^s = \int_0^L \left[-N_{x,x}^s \delta u_0 - M_{x,xx}^s \delta w_0 \right.$$
$$\left. + (M_{x2}^s - M_{x1,x}^s) \delta \phi \right] dx \quad (23)$$

where

$$(N_x^s, M_x^s, M_{x1}^s) = b \int \sigma_x^s (1, z, R) dz \quad (24a)$$

$$M_{x2}^s = b \int \frac{1}{2} \sigma_{xz}^s \frac{\partial R}{\partial z} dz \quad (24b)$$

4.4 The variation of kinetic energy

The variation of the kinetic energy of the micro composite sinusoidal beams can be given by Simsek and Reddy (2013)

$$\delta T = \int_\forall \rho \left[(\frac{\partial u}{\partial t})(\frac{\partial \delta u}{\partial t}) + (\frac{\partial w}{\partial t})(\frac{\partial \delta w}{\partial t}) \right] d\forall \quad (25)$$

where ρ is the mass density of sinusoidal micro composite beam. By using Eqs. (6a)-(6c) and Eq. (25), the first variation of the kinetic energy is given by

$$\delta T = -b \int_0^L \begin{bmatrix} (I^{(0)} \frac{\partial^2 u_0}{\partial t^2} - I^{(1)} \frac{\partial^3 w_0}{\partial x \partial t^2} + I^{(3)} \frac{\partial^2 \phi_x}{\partial t^2}) \delta u_0 \\ +(I^{(1)} \frac{\partial^3 u_0}{\partial x \partial t^2} + I^{(0)} \frac{\partial^2 w_0}{\partial t^2} - I^{(2)} \frac{\partial^4 w_0}{\partial x^2 \partial t^2} + I^{(4)} \frac{\partial^3 \phi_x}{\partial x \partial t^2}) \delta w_0 \\ +(I^{(3)} \frac{\partial^2 u_0}{\partial t^2} - I^{(4)} \frac{\partial^3 w_0}{\partial x \partial t^2} + I^{(5)} \frac{\partial^2 \phi_x}{\partial t^2}) \delta \phi_x \end{bmatrix} dx \quad (26)$$

where

$$(I^{(0)}, I^{(1)}, I^{(2)}) = \int_{-\frac{h}{2}}^{\frac{h}{2}} \rho(1, z, z^2) dz \quad (27a)$$

$$(I^{(3)}, I^{(4)}, I^{(5)}) = \int_{-\frac{h}{2}}^{\frac{h}{2}} \rho R(z)(1, z, R(z)) dz \quad (27b)$$

4.5 The variation of work done due to the external work

In this study, the work done due to the external forces are considered as follows:

(a) The effects of elastic foundation;
(b) The effects of magnetic field in z direction;
(c) The effects of external Load $q(x)$;
(d) The effects of temperature changes;
(e) The effects of axial buckling load.

In this section, the first variation of components of work done due to the external forces is described (Mohammadimehr *et al.* 2015)

$$V^{elastic} = \frac{1}{2} \int_0^L F^{elastic} w_0 dx \quad (28a)$$

$$F^{elastic} = k_w w_0 - k_g \nabla^2 w_0 \quad (28b)$$

where $V^{elastic}$ denotes the work done due to the elastic foundation and it is defined as

$$\overrightarrow{H} = (0, 0, H_z) \quad (29)$$

The Maxwell relations and variation of external work done by magnetic field for the micro composite beams can be expressed as (Mohammadimehr *et al.* 2014)

$$\overrightarrow{H} = (0, 0, H_z) \quad (30a)$$

$$\overrightarrow{h} = \nabla \times (\overrightarrow{U} \times \overrightarrow{H}) \quad (30b)$$

$$\overrightarrow{j} = \overrightarrow{\nabla} \times \overrightarrow{h} \quad (30c)$$

$$\overrightarrow{f_l} = \eta(\overrightarrow{j} \times \overrightarrow{H}) \quad (30d)$$

where $\overrightarrow{H}$, $\overrightarrow{h}$, $\overrightarrow{U}$, $\overrightarrow{J}$, $\overrightarrow{f_l}$ and η are magnetic intensity vector, perturbation of magnetic field vector, displacement vector, electric current density vector, Lorentz forces and magnetic permeability, respectively. Substituting Eqs. (6a)-(6c) into Eq. (30) yields the following equation

$$\delta V^{fl} = \int_\forall (f_{xl} \delta u + f_{zl} \delta w) d\forall \quad (31)$$

and finally, the first variation of magnetic external works is defined as

$$\delta V^{fl} = b \int_0^L \begin{bmatrix} (Y^{(1)} u_{0,xx} + Y^{(3)} \phi_{xx} + Y^{(5)} \phi) \delta u_0 \\ +(Y^{(4)} \phi_{xxx} - Y^{(2)} w_{0,xxxx} + Y^{(6)} \phi_x) \delta w_0 \\ +(Y^{(3)} u_{0,xx} - Y^{(4)} w_{0,xxx} + Y^{(3)} \phi_{xx} + Y^{(7)} \phi) \delta \phi \end{bmatrix} dx \quad (32)$$

where

$$(Y^{(1)}, Y^{(2)}) = \int_{-\frac{h}{2}}^{\frac{h}{2}} \eta H_z^2 (1, z^2) dz \tag{33a}$$

$$(Y^{(3)}, Y^{(4)}) = \int_{-\frac{h}{2}}^{\frac{h}{2}} \eta H_z^2 R(z)(1, z) dz \tag{33b}$$

$$(Y^{(5)}, Y^{(6)}, Y^{(7)}) = \int_{-\frac{h}{2}}^{\frac{h}{2}} \eta H_z^2 \frac{\partial^2 R(z)}{\partial z^2}(1, z, R(z)) dz \tag{33c}$$

The external applied force $q(x)$ and axial buckling load can be expressed by

$$\delta V = b\delta \int_0^L (\frac{1}{2} N_{x_0} (\frac{\partial w_0}{\partial x})^2 - q(x) w_0) dx \tag{34}$$

4.6 The governing equations of micro composite sinusoidal beams

In this work, Hamilton's principle is used to derive the governing equations of motion. According to Hamilton's principle, the actual motion minimizes the difference of the kinetic and total potential energy for a system with prescribed configurations at $t = 0$ and $t = T$ that is (Ma *et al.* 2008, Ebrahimi and Barati 2016b)

$$\delta \int_{t_1}^{t_2} \prod dt = 0 \rightarrow \int_{t_1}^{t_2} [\delta T - (\delta U + \delta U^s + \delta V^{elastic} + \delta V^{fl} + \delta V)] dt = 0 \tag{35}$$

where T, U, U^s, $V^{elastic}$, V^{fl} and V are the kinetic energy, total potential energy, surface energy and work done by elastic medium foundation, magnetic field and the effects of external and axial buckling loads, respectively.

Substituting Eqs. (12), (23), (26), (29), (32) and (34) into Eq. (35), the governing equations of motion are derived.

δu_0 :

$$\begin{cases} -(A_{11} + A_0^s + A_1^s - Y^{(1)})u_{0,xx} + (P^{(0)} + \frac{5}{2}T^{(0)})u_{0,xxxx} + (B_{11} + B_0^s + B_1^s - q_z^{(1)}\tau^s)w_{0,xxx} \\ -(P^{(1)} + \frac{5}{2}T^{(1)})w_{0,xxxxx} + Y^{(5)}\phi_x - (B_{11} + B_0^{'s} + B_1^{'s} + \frac{5}{4}T^{(3)} - Y^{(3)})\phi_{x,xx} \\ +(P^{(2)} + \frac{5}{2}T^{(2)})\phi_{x,xxxx} + I^{(0)}u_{0,tt} + (q_z^{(1)}\rho^s - I^{(1)})w_{0,xtt} + I^{(3)}\phi_{x,tt} + N_x^T + N_{0,x}^{sT} + N_{1,x}^{sT} = 0 \\ \text{Boundary condition at } x = 0 \text{ and } x = L : \\ [N_x + \frac{\partial}{\partial x}(P_x^{(0)} + T_{xxx}^{(0)} - T_{xyy}^{(0)} - T_{xzz}^{(0)})]\Big|_0^L = 0 \end{cases} \tag{36a}$$

δw_0 :

$$\begin{cases} -(B_{11} + B_0^s + B_1^s)u_{0,xxx} + (P^{(1)} + \frac{5}{2}T^{(1)})u_{0,xxxxx} + bk_w w_0 + (Y^{(3)} - bk_g + N_{x0})w_{0,xx} \\ +(D_{11} + D_0^s + D_1^s - q_z^{(2)}\tau^s + P^{(0)} + \frac{5}{3}T^{(0)} + M^{(0)} - Y^{(2)})w_{0,xxxx} - (P^{(3)} + \frac{5}{2}T^{(4)})w_{0,xxxxxx} \\ +Y^{(6)}\phi_{x,x} - (B_{11}^{'} + D_0^{'s} + D_1^{'s} + P^{(6)} + \frac{5}{2}T^{(6)} + \frac{8}{3}T^{(0)} + \frac{2}{3}T^{(10)} + \frac{1}{2}M^{(0)} - Y^{(4)})\phi_{x,xxx} \\ +(P^{(4)} + \frac{5}{2}T^{(5)})\phi_{x,xxxxx} + M_{,xx}^T + M_{0,xx}^{sT} + M_{1,xx}^{sT} - bq(x) + I^{(1)}u_{0,xtt} + I^{(0)}w_{0,tt} \\ +(q_z^{(2)}\rho^s - I^{(2)})w_{0,xxtt} + I^{(4)}\phi_{x,xtt} = 0 \\ \text{Boundary condition at } x = 0 \text{ and } x = L : \\ -[\frac{\partial^2}{\partial x^2}(P_x^{(1)} + T_{xxx}^{(1)} + \frac{3}{4}T_{xzz}^{(1)} - +T_{xyy}^{(1)} - T_{zzz}^{(1)}) + \frac{\partial}{\partial x}(P_z^{(0)} + M_x^{(0)} + M_{xy}^{(0)} - T_{yyz}^{(0)} - T_{zzz}^{(0)})]\Big|_0^L = 0 \end{cases} \tag{36b}$$

$\delta\phi_x$:

$$\begin{cases} -(B_{11}^{'} + B_0^{'s} + B_1^{'s} + \frac{5}{4}T^{(3)} - Y^{(3)})u_{0,xx} + (P^{(2)} + \frac{5}{2}T^{(2)})u_{0,xxxx} + (B_2^s + B_3^s)w_{0,x} \\ +(B_{11}^{'} + D_0^{'s} + D_1^{'s} + P^{(7)} + \frac{5}{4}T^{(6)} + \frac{10}{3}T^{(10)} + \frac{1}{2}M^{(1)} - Y^{(4)} - q_z^{(3)}\tau^s)w_{0,xxx} \\ -(P^{(4)} + \frac{5}{2}T^{(5)})w_{0,xxxxx} + (D_{55}^R + \frac{5}{3}T^{(9)} + \frac{1}{4}M^{(3)} + Y^{(7)})\phi_x - (B_{11}^R + R_0^s + R_1^s) \\ +P^{(8)} + \frac{5}{2}T^{(8)} + \frac{20}{3}T^{(11)} + \frac{1}{4}M^{(2)} - Y^{(3)})\phi_{x,xx} + (P^{(5)} + \frac{5}{2}T^{(7)})\phi_{x,xxxx} + N_{R,x}^T \\ +M_{0,x}^{'sT} + M_{1,x}^{'sT} + I^{(3)}u_{0,tt} + (q_z^{(3)}\rho^s - I^{(4)})w_{0,xtt} + I^{(5)}\phi_{x,tt} = 0 \\ \text{Boundary condition at } x = 0 \text{ and } x = L : \\ [M_x^{(0)} + P_z^{(1)} + M_{xy}^{(1)} + \frac{3}{4}T_{xzz}^{(1)} - T_{yyz}^{(1)} - T_{zzz}^{(1)} + \frac{\partial}{\partial x}(P_x^{(2)} + T_{xxx}^{(2)} - T_{xyy}^{(2)} - T_{xzz}^{(2)})]\Big|_0^L = 0 \end{cases} \tag{36c}$$

where

$$(A_{11}, B_{11}, D_{11}) = \int_{-\frac{h}{2}}^{\frac{h}{2}} C_{11}(1, z, z^2) dz \tag{37a}$$

$$(B_{11}^{'}, B_{11}^{"}, B_{11}^R) = \int_{-\frac{h}{2}}^{\frac{h}{2}} C_{11}(1, z, R) R dz \tag{37b}$$

$$D_{55}^R = K_s \int_{-\frac{h}{2}}^{\frac{h}{2}} C_{55}(\frac{\partial R}{\partial z})^2 dz \tag{37c}$$

$$(q_z^{(1)}, q_z^{(2)}, q_z^{(3)}) = \int_{-\frac{h}{2}}^{\frac{h}{2}} \frac{\upsilon}{1-\upsilon}(1, z, R)(\frac{2z}{h}) dz \tag{37d}$$

$$(A_0^s, B_0^s, D_0^s, B_0^{'s}, D_0^{'s}, R_0^s) = \int_{-t-\frac{h}{2}}^{-\frac{h}{2}} E^s (1, z, z^2, R, Rz, R^2) dz \tag{37e}$$

$$(A_1^s, B_1^s, D_1^s, B_1^{'s}, D_1^{'s}, R_1^s) = \int_{\frac{h}{2}}^{t+\frac{h}{2}} E^s (1, z, z^2, R, Rz, R^2) dz \tag{37f}$$

$$(A_0^{'s}, B_0^{"s}, B_2^s) = \int_{-t-\frac{h}{2}}^{-\frac{h}{2}} \tau^s (1, z, \frac{\partial R}{\partial z}) dz \tag{37g}$$

$$(A_1^{'s}, B_1^{"s}, B_3^s) = \int_{\frac{h}{2}}^{t+\frac{h}{2}} \tau^s (1, z, \frac{\partial R}{\partial z}) dz \tag{37h}$$

where t is the thickness of surface layer that it is considered $0.1 \times h$.

Also, K_s is the shear correction factor that it is equal to 1 for the classic (Euler-Bernoulli model) and higher order shear deformation theories such as sinusoidal beam models while this parameter is equal to 5/6 for Timoshenko beam theory. Thus, it is noted that in the Eq. (37c), this parameter is introduced.

5. Solution method

In this article, Navier's type solution is employed to obtain the static, buckling and free vibration of the micro composite sinusoidal beam reinforced by SWCNTs embedded in an elastic foundation for two edges simply

supported boundary conditions. The simply supported boundary conditions of micro composite beams at $x = 0$ and $x = L$ are given as (Lei *et al.* 2013a)

$$u_{0,x}(x = 0, L) = 0 \tag{38a}$$

$$\phi_{x,x}(x = 0, L) = 0 \tag{38b}$$

$$w_0(x = 0, L) = 0 \tag{38c}$$

$$w_{0,xx}(x = 0, L) = 0 \tag{38d}$$

the following expansion of the displacement field is defined as follows (Ebrahimi and Barati 2016a)

$$u_0(x,t) = \sum_{m=1}^{\infty} U_m \cos(\frac{m\pi}{L}x)e^{i\omega t} \tag{39a}$$

$$w_0(x,t) = \sum_{m=1}^{\infty} W_m \sin(\frac{m\pi}{L}x)e^{i\omega t} \tag{39b}$$

$$\phi_x(x,t) = \sum_{m=1}^{\infty} \phi_m \cos(\frac{m\pi}{L}x)e^{i\omega t} \tag{39c}$$

where U_m, W_m and ϕ_m are the undetermined Fourier coefficients, respectively. Also, ω is the vibration frequency, m is transverse wave number and $i = \sqrt{-1}$.

Substituting Eq. (52) into Eq. (49) yields

$$\left(\begin{bmatrix} k_{11} & k_{12} & k_{13} \\ k_{21} & k_{22} & k_{23} \\ k_{31} & k_{32} & k_{33} \end{bmatrix} - \zeta_1\omega^2 \begin{bmatrix} M_{11} & M_{12} & M_{13} \\ M_{21} & M_{22} & M_{23} \\ M_{31} & M_{32} & M_{33} \end{bmatrix} - \zeta_2 N_x \begin{bmatrix} N_{11} & N_{12} & N_{13} \\ N_{21} & N_{22} & N_{23} \\ N_{31} & N_{32} & N_{33} \end{bmatrix} \right) \begin{Bmatrix} U_m \\ W_m \\ \phi_m \end{Bmatrix} = \zeta_3 \begin{Bmatrix} f_1 \\ f_2 \\ f_3 \end{Bmatrix} \tag{40}$$

where K_{ij}, M_{ij}, N_{ij} and f_i are shown in Appendix B.

Also, the external applied force $q(x)$ and temperature changes are expanded by Fourier series as follows

$$\begin{cases} q(x) = \sum_{m=1}^{\infty} q_m \sin(\frac{m\pi}{L}x) \\ q_m = \frac{2}{L}\int_0^L q(x)\sin(\frac{m\pi}{L}x)dx \quad ; \quad q(x) = q_0 \end{cases} \rightarrow q_m = \frac{4q_0}{n\pi}, \tag{41a}$$

$$n = 1,3,5,...$$

$$N^T = \sum_{m=1}^{\infty} N_m^T \sin(\frac{m\pi}{L}x) \tag{41b}$$

$$N_m^T = \frac{2}{L}\int_0^L N^T \sin(\frac{m\pi}{L}x)dx \quad ; \quad N^T = b\int_{-\frac{h}{2}}^{\frac{h}{2}} C_{11}\alpha_{11}\Delta T dz$$

Table 2 The amounts of ζ coefficient in various analyses of micro composite sinusoidal beam reinforced by carbon nanotubes (CNTs)

	ζ_1	ζ_2	ζ_3
Bending analysis	0	0	1
Buckling analysis	0	1	0
Free vibration analysis	1	0	0

and the other parameters are determined similarly.

In Eq. (40), the ζ coefficients used for the static, buckling and free vibration analysis of micro composite sinusoidal beam reinforced by SWCNTs in which the amount of ζ coefficient in various analyses is shown in Table 2.

6. Validation

6.1 The validation of static bending and buckling analysis of micro sinusoidal beams

In this section, the dimensionless maximum deflection and critical buckling loads for FG micro beams are compared with the obtained results calculated by numerical solution methods to establish the validity and accuracy of the present solution method. In order to validate the effects of these behaviors, the obtained results are compared with the reported results by Akgöz and Civalek (2015a) based on modified strain gradient theory (MSGT) for static analysis and with the presented results by them (Akgöz and Civalek 2015a) based on modified couple stress theory (MCST) for buckling analysis. Also, numerical examples are presented to investigate the deflection and buckling behaviors of FG microbeams. It is assumed that the material properties vary smoothly along the thickness of FG micro beam. For this purpose, the following material and geometric parameters are used (Akgöz and Civalek 2014b, 2015b)

$$Metal \begin{cases} E_m = 70 Gpa \\ \upsilon_m = 0.23 \end{cases} \qquad Cramic \begin{cases} E_c = 380 Gpa \\ \upsilon_c = 0.23 \end{cases}$$

Tables 3 and 4 give the maximum dimensionless deflection of the FG micro beam subjected to uniform transverse load without elastic foundation and dimensionless critical buckling loads of FG micro beams for simply supported edges. It is seen that results agree well with each other.

$$\overline{W} = \frac{1000wE_mI}{q_0L^4} \tag{42a}$$

$$\overline{p_{cr}} = \frac{p_{cr}L^2}{EI} \tag{42b}$$

where

$$E = E_m + (E_c - E_m)V_c \tag{43a}$$

$$V_c = (\frac{1}{2} + \frac{z}{h})^k \tag{43b}$$

$$I = b\int_{-\frac{h}{2}}^{\frac{h}{2}} z^2 dz \tag{43c}$$

6.2 The validation of free vibration analysis of micro sinusoidal beams

In this article, in order to display the efficiency of the present model, the results of this model are carried out

Table 3 The comparison of the maximum deflection for
FG micro beam with $q_0 = 10\ \mu\text{N/m}$, $l = 15\ \mu m$, $L = 6h$
based on MSGT

	$\dfrac{h}{l}$	Maximum dimensionless deflection		
		$k = 0.5$	$k = 1.0$	$k = 2.0$
Present work		0.1972	0.2422	0.3098
Akgöz and Civalek 2015a	1	0.1940	0.2382	0.3050
Present work		0.9693	1.2043	1.5477
Akgöz and Civalek 2015a	2.5	0.9571	1.1892	1.5280
Present work		2.2210	2.8108	3.6206
Akgöz and Civalek 2015a	5	2.2019	2.7864	3.5877

Table 4 The comparison of the first dimensionless buckling load
for FG micro beam with $l = 15\ \mu m$ and $L = 10h$ based on
MCST

	$\dfrac{h}{l}$	Maximum dimensionless deflection		
		$k = 0.3$	$k = 0.6$	$k = 0.9$
Present work		249.7506	211.7566	186.3461
Akgöz and Civalek 2014b	1	249.7506	211.7576	186.3461
Present work		52.5767	43.1523	37.2388
Akgöz and Civalek 2014b	4	52.5768	43.1523	37.2388
Present work		42.7179	34.7220	29.7835
Akgöz and Civalek 2014b	8	42.7180	34.7220	29.7834

Table 5 The comparison of the first dimensionless natural
frequency for homogenous micro beam whit $l = 17.6\ \mu m$
and $L = 10h$ based on CT, MCST and MSGT

	Dimensionless natural frequencies $(\bar{\omega})$		
	CT	MCST	MSGT
Present work	0.2791	0.3828	0.5617
Lei *et al.* 2013c	0.2790	0.3827	0.5625
Ansari *et al.* 2011	0.2854	0.3863	0.5430

which are compared with the results of the previously papers. Table 5 demonstrates the comparison of the first dimensionless natural frequencies of the homogenous micro beam for classical theory (CT), MCST and MSGT. In this study, based on the MSGT, the static, buckling and free vibration analysis of the micro composite sinusoidal beams reinforced by SWCNTs is presented. If the material length scale parameters (l_0, l_1) are equal to zero, the model is named as the MCST while, for all the material length scale parameters are equal to zero, it is said the CT. Also, the following first dimensionless natural frequency can be defined as (Lei *et al.* 2013c)

$$\bar{\omega} = \omega L \sqrt{\frac{I_{10}}{A_{110}}} \tag{44}$$

where

$$I_{10} = \int_{-\frac{h}{2}}^{\frac{h}{2}} \rho \, dz \tag{45a}$$

$$A_{110} = \int_{-\frac{h}{2}}^{\frac{h}{2}} \frac{E(1-\upsilon)}{(1+\upsilon)(1-2\upsilon)} \, dz \tag{45b}$$

$$Metal\,(AL) \begin{cases} E = 70Gpa \\ \rho = 2720Kg\,/\,m^3 \\ \upsilon = 0.3 \end{cases} \tag{45c}$$

In Table 5, there are some small differences of the first dimensionless natural frequency between the present results and the obtained results by Ansari *et al.* (2011), which it is due to the effect of the sinusoidal shear deformation.

7. Numerical results and discussion

In this study, based on modified strain gradient theory (MSGT), the effects of length scale parameter, surface stresses, magnetic field and temperature changes on the bending, buckling and free vibration behaviors of the micro composite sinusoidal beam reinforced by SWCNTs embedded in an elastic medium are presented. It is assumed that the material length scale parameter of micro beam to be $l = 17.6\ (\mu m)$. Also, the used parameters in this section are considered as the following form: $h = 2l$, $4l$, $b = h$, $\tau^s = 1.7$ (N/m), $\rho^s = 7\ (\mu \text{Kg/m}^3)$, $k_w = 600\ (\text{GN/m}^3)$, $k_g = 1000$ (N/m), $\Delta T = 20$ and $H_z = 0.02\ (\text{A}/\mu m)$.

Table 6 offers the effect of surface layer thickness on the static, buckling and free vibration responses of micro beam. The results of this Table show that the surface stresses layer causes decrease the maximum deflection while increase the dimensionless natural frequencies and critical buckling load

Table 6 Comparison of surface stresses effect on the static,
buckling and free vibration behavior of micro composite
beam reinforced by SWCNT for $L = 10h$, $\Delta T = 30$,
$E^s = -3$ N/μm and, $k_w = k_g = 0$

	$\dfrac{h}{l}$	$t = 0$	$t = 0.05h$	$t = 0.1h$	$t = 0.15h$
	2	0.340154	0.319821	0.298160	0.274909
$\bar{W}_{max}$	4	0.482693	0.462097	0.437992	0.409947
	8	0.579695	0.569682	0.556608	0.539251
	2	379.2580	403.3694	432.6744	469.2680
$\bar{P}_{cr}$	4	267.2633	279.1755	294.5402	314.6897
	8	222.5412	226.4527	231.7720	239.2319
	2	1.385489	1.428674	1.479480	1.540621
$\bar{\omega}$	4	1.163980	1.189589	1.221845	1.262943
	8	1.062435	1.071748	1.084308	1.101737

Table 7 The effects of surface stresses on the bending behavior of micro beam reinforced by SWCN in presence of magnetic field and temperature changes for $h = 4l$ and $L = 10h$

k_w (GN/m³) k_g (N/m)	H_z (A/μm)	ΔT	Dimensionless maximum deflection $(\overline{W}_{0max})$		
			$E^s = -50$	$E^s = 0.0$	$E^s = 50$
$k_w = 0.0$ $k_g = 0.0$	0.0	0	0.454866	0.453187	0.451523
		25	0.442099	0.440463	0.438842
	0.02	0	0.381322	0.380125	0.378939
		25	0.368093	0.366949	0.365815
$k_w = 600$ $k_g = 0.0$	0.0	0	0.269177	0.268588	0.268003
		25	0.258505	0.257944	0.257388
	0.02	0	0.241602	0.241121	0.240643
		25	0.231312	0.230859	0.230410
$k_w = 0.0$ $k_g = 1000$	0.0	0	0.439155	0.437590	0.436039
		25	0.426395	0.424872	0.423364
	0.02	0	0.370219	0.369091	0.367972
		25	0.357141	0.356064	0.354996
$k_w = 600$ $k_g = 1000$	0.0	0	0.263596	0.263032	0.262470
		25	0.253055	0.252518	0.251984
	0.02	0	0.237097	0.236634	0.236173
		25	0.226939	0.226503	0.226071

Table 8 The effects of surface stresses on the buckling analysis of micro beam reinforced by SWCNTs in presence of magnetic field and temperature changes for $h = 4l$ and $L = 10h$

k_w (GN/m³) k_g (N/m)	H_z (A/μm)	ΔT	Dimensionless maximum deflection $(\overline{P}_{cr})$		
			$E^s = -50$	$E^s = 0.0$	$E^s = 50$
$k_w = 0.0$ $k_g = 0.0$	0.0	0	284.5594	284.6643	284.7693
		25	292.7792	292.8875	292.9958
	0.02	0	339.2716	339.3779	339.4843
		25	351.4548	351.5460	351.6731
$k_w = 600$ $k_g = 0.0$	0.0	0	480.2077	480.3127	480.4176
		25	500.0233	500.1316	500.2399
	0.02	0	534.9199	535.0262	535.1326
		25	558.6990	558.8081	558.9172
$k_w = 0.0$ $k_g = 1000$	0.0	0	294.7055	294.8104	294.9154
		25	303.5266	303.6349	303.7432
	0.02	0	349.4177	349.5240	349.6304
		25	362.2023	362.3114	362.4206
$k_w = 600$ $k_g = 1000$	0.0	0	490.3538	490.4588	490.5637
		25	510.7708	510.8791	510.9873
	0.02	0	545.0660	545.1723	545.2787
		25	569.4464	569.5556	569.6647

of microbeam because the surface layer lead to increase the stiffness of micro structure. In this article, for most realistic results the surface stresses are considered.

Tables 7-9 investigated the effects of surface Lame constant on dimensionless maximum deflection, critical buckling load and natural frequencies of micro composite sinusoidal beam reinforced by single-walled carbon nano-

tubes (SWCNTs) based on MSGT in presence of magnetic field and temperature changes. It is shown that increasing the surface Lame constant lead to increase the stiffness of micro structure. Thus, it is demonstrated that by increasing the surface Lame constant, the dimensionless maximum deflection reduces while increase the dimensionless buckling load and natural frequencies. Also, the presence or

Table 9 The effects of surface stresses on the free vibration response of micro composite beam
reinforced by SWCNTs in presence of magnetic field and temperature changes for $h = 4l$
and $L = 10h$

k_w (GN/m³) k_g (N/m)	H_z (A/μm)	ΔT	Dimensionless maximum deflection $(\overline{\omega})$		
			$E^s = -50$	$E^s = 0.0$	$E^s = 50$
$k_w = 0.0$ $k_g = 0.0$	0.0	0	1.20091	1.20107	1.20123
		25	1.21820	1.21836	1.21853
	0.02	0	1.31126	1.31141	1.31156
		25	1.33469	1.33484	1.33499
$k_w = 600$ $k_g = 0.0$	0.0	0	1.56001	1.56014	1.56026
		25	1.59196	1.59209	1.59222
	0.02	0	1.64646	1.64658	1.64670
		25	1.68277	1.68290	1.68302
$k_w = 0.0$ $k_g = 1000$	0.0	0	1.22212	1.22229	1.22245
		25	1.24035	1.24051	1.24068
	0.02	0	1.33072	1.33087	1.33102
		25	1.35494	1.35509	1.35524
$k_w = 600$ $k_g = 1000$	0.0	0	1.5764	1.57653	1.57665
		25	1.60898	1.60911	1.60923
	0.02	0	1.66200	1.66212	1.66224
		25	1.69888	1.69900	1.69912

(a) Maximum deflection (b) First critical buckling load (c) First natural frequencies
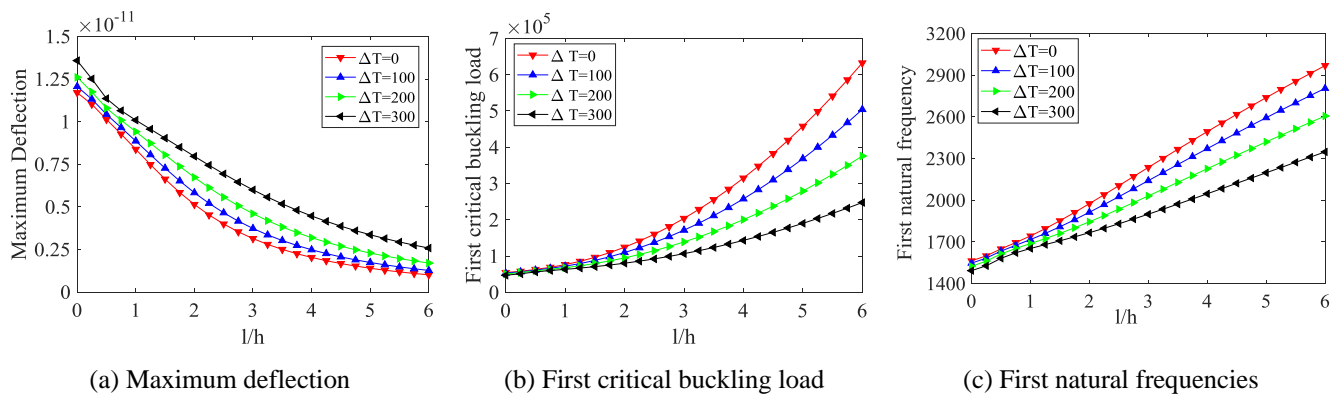
Fig. 2 Effect of temperature changes on the static, buckling and vibration of micro composite sinusoidal beam for $L = 10h$

Table 10 The effects of surface stresses on the static, buckling, and free vibration response of
micro sinusoidal beam in presence of magnetic field for $h = 4l$, $L = 10h$ and $q_0 = 10N$

	ΔT	$E^s = -50$ (N/μm)	$E^s = 0.0$	$E^s = 50$ (N/μm)
$W_{max}(10^{-12})$	0	7.63045	7.61555	7.60074
	40	7.80404	7.78925	7.77455
	80	8.00223	7.98762	7.97310
P_{cr}	0	53721.702	53732.186	53742.668
	40	52527.024	52533.97	52543.914
	80	51219.965	51229.308	51238.649
ω	0	3216899.8	3217133.2	3217366.6
	40	3181206.3	3181429.6	3181652.8
	80	3141866.4	3142078.1	3142289.8

(a) Dimensionless maximum deflection

(b) Dimensionless first critical
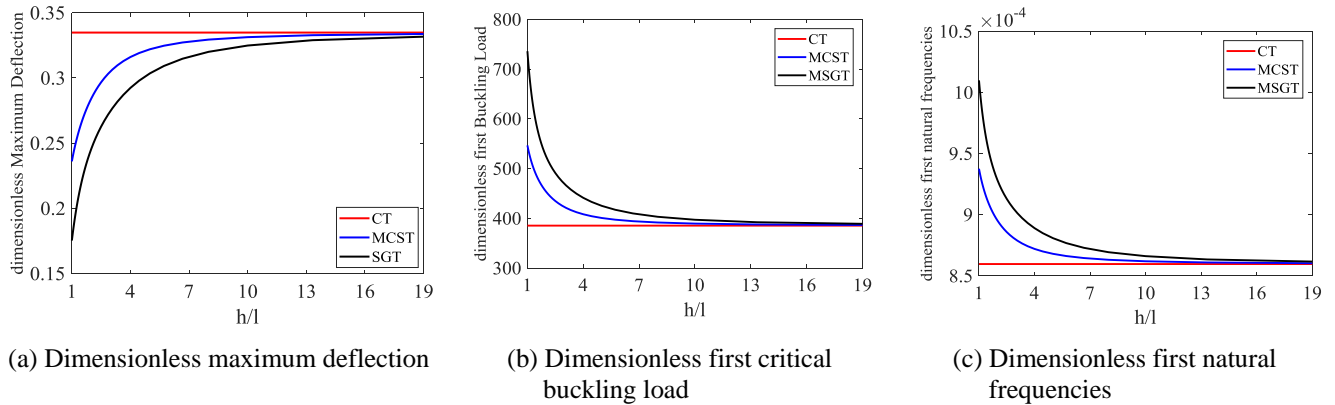buckling load

(c) Dimensionless first natural
frequencies

Fig. 3 Effects of material length scale parameter on the static, buckling and vibration of micro beam for $L = 10h$
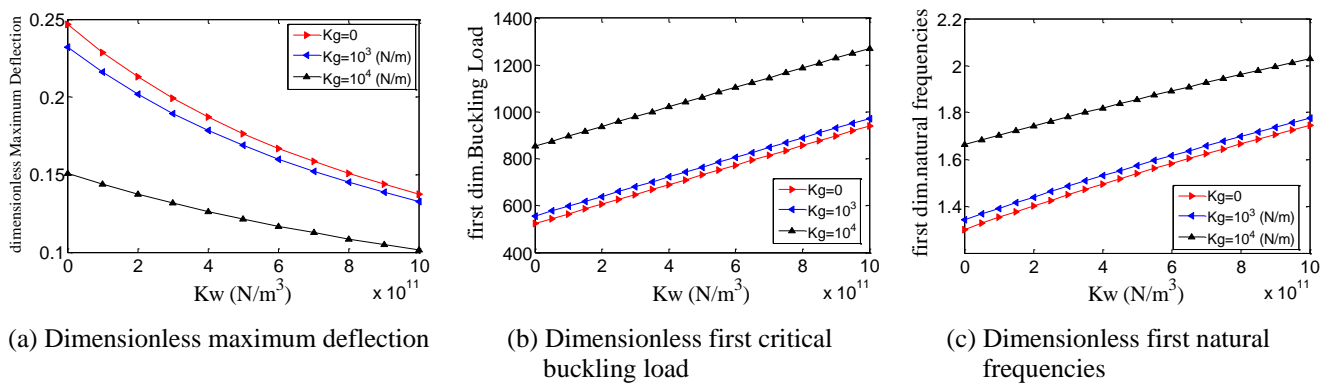and $k_w = k_g = 0$

(a) Dimensionless maximum deflection

(b) Dimensionless first critical
buckling load

(c) Dimensionless first natural
frequencies

Fig. 4 Effects of elastic medium on the static, buckling and vibration of micro composite sinusoidal beam for $L = 10h$

absence of elastic foundation, magnetic field and temperature changes on surface Lame constant are considered. It is clear that the effects of elastic medium and magnetic field increase the dimensionless critical buckling load and natural frequencies and decreases the dimension-less maximum deflection because these parameters increase the stiffness of micro beam.

Moreover, it is known that rising temperature lead to reduce the stiffness of structures. Therefore, it is expected that increasing the temperature changes lead to reduce the critical buckling load and natural frequencies and increases the deflection of micro beam which it is shown in Fig. 2, Table 10.

Fig. 3 illustrates the effects of material length scale parameters on the dimensionless maximum deflection, the critical buckling load and the natural frequency of the micro composite sinusoidal beam reinforced by SWCNTs based on CT, MCST and MSGT, respectively. It is shown that considering material length scale parameters lead to increase stiffness of micro structure, therefore reduces the dimensionless maximum deflection while increase the dimensionless critical buckling load and the dimensionless natural frequencies. Also, it is presented that the effect of material length scale parameters is noticeable for lower values of thickness-to-material length scale parameters. So that, the various size dependent effects including CT, MCST and MSGT are converged by increasing the thickness-to-

material length scale parameters $\left(\frac{h}{l} > 20 \right)$.

Fig. 4 illustrates the effect of different values of elastic foundation on the static bending, buckling and free vibration analyses of micro composite sinusoidal beam reinforced by SWCNTs. It is shown that with increasing the Winkler spring constant (k_w) decreases the maximum deflection of micro composite beam because the strength of micro beam increases under various loads with increasing the stiffness of structure [Fig. 4(a)]. Thus, this increases the stiffness causes to increase the dimensionless critical buckling load and natural frequencies. Then, it can be seen that the resonance phenomena delays [Figs. 4(a) and 3(b)]. Also, it is shown that the Pasternak shear modulus has greater influence on the behaviors of micro beam. So that the effect of Pasternak shear modulus is more important than Winkler spring constant.

Fig. 5 shows the effect of composite fiber angle on the dimensionless maximum deflection, critical buckling load and natural frequency of micro composite sinusoidal beam based on MSGT. It is observed from this figure that with increasing the composite fiber angle, the dimensionless maximum deflection of micro beam reduces while the dimensionless natural frequency and the dimensionless critical buckling load increase.

Fig. 6 shows the effects of magnetic field on the static bending, buckling and free vibration responses of micro composite sinusoidal beam reinforced by SWCNTs based
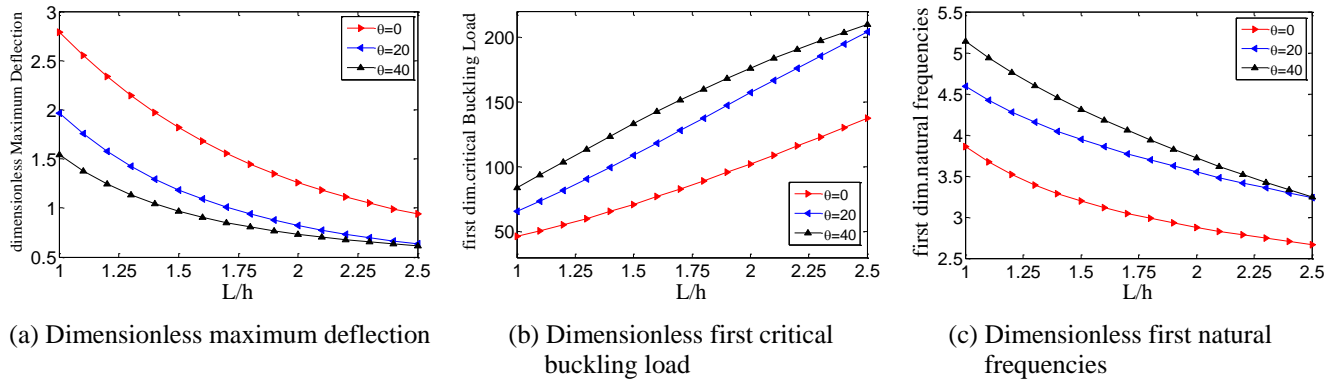
(a) Dimensionless maximum deflection

(b) Dimensionless first critical buckling load

(c) Dimensionless first natural frequencies

Fig. 5 Effects of composite fiber angle on the behaviors of micro composite sinusoidal beam for $k_w = k_g = 0$, and $H_z = 0$
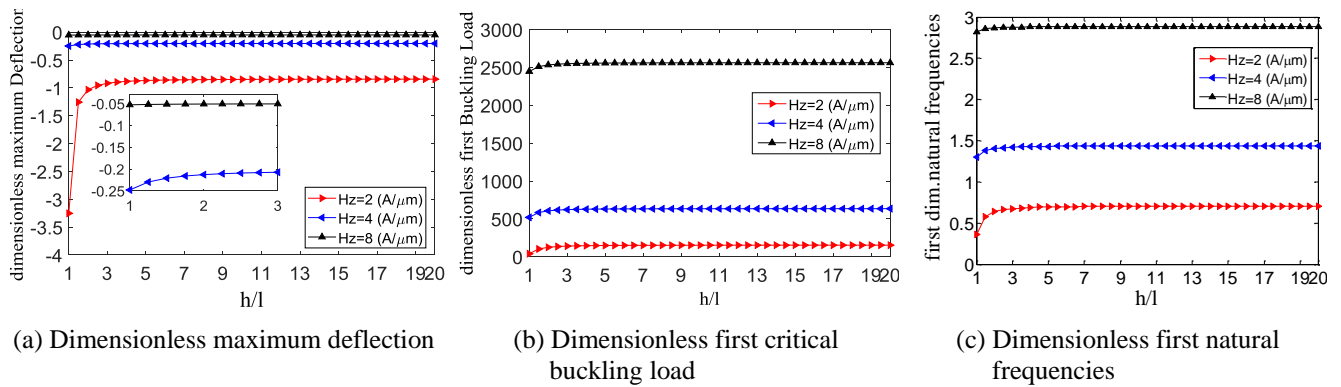

(a) Dimensionless maximum deflection

(b) Dimensionless first critical buckling load

(c) Dimensionless first natural frequencies

Fig. 6 Effects of magnetic field on the behaviors of micro composite sinusoidal beam $L = 10h$ and $k_w = k_g = 0$

(a) Maximum deflection

(b) First critical buckling load
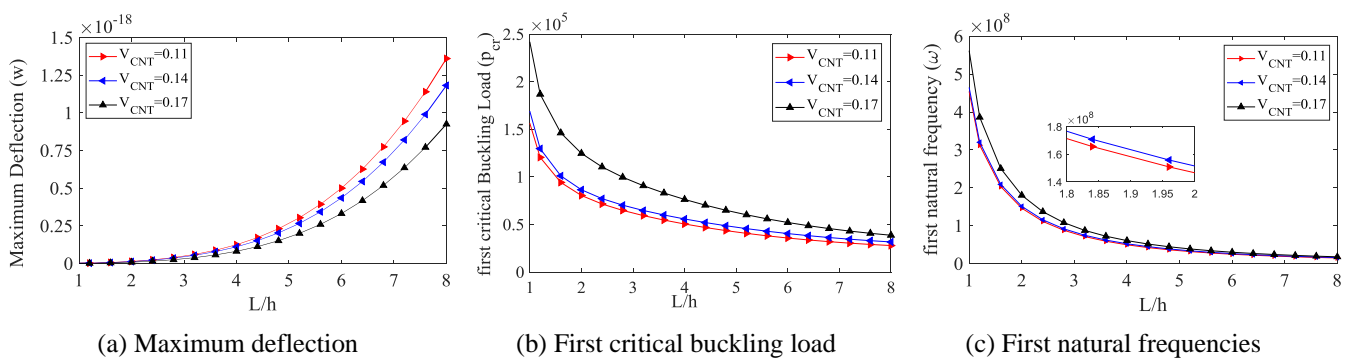
(c) First natural frequencies

Fig. 7 Effects of carbon nanotubes volume fraction on the behaviors of micro composite sinusoidal beam for $h = l$

on MSGT. It is demonstrated that the effect of magnetic field is much greater than material length scale parameter and elastic foundation. The magnetic field due to the presence of carbon nanotubes is caused to create a resistance force against structural deformation and thus it increases the stiffness of micro composite beam. Therefore, it is observed from this figure that increasing the magnetic intensity lead to increase the dimensionless critical buckling load and dimensionless natural frequency while the dimensionless maximum deflection reduces because the stiffness of micro structure increases by increasing the magnetic intensity.

Fig. 7 shows the influence of carbon nanotube volume fraction on the maximum deflection, first critical buckling

load and first natural frequencies of the micro composite sinusoidal beam embedded in an elastic medium in presence of magnetic field versus length-to-thickness ratio. It is noticeable that increasing the carbon nanotube volume fraction lead to increase stiffness of micro beam. Thus, it can be seen that the critical buckling load and natural frequencies increasing with increasing of SWCNT volume fraction while decreases the dimensionless maximum deflection. Also, it is noted that in this figure the maximum deflection, first critical buckling load and first natural frequencies of micro beam are depicted because of there are L/h parameter in the Eq. (42). Thus, it is necessary do not curve as dimensionless parameter.
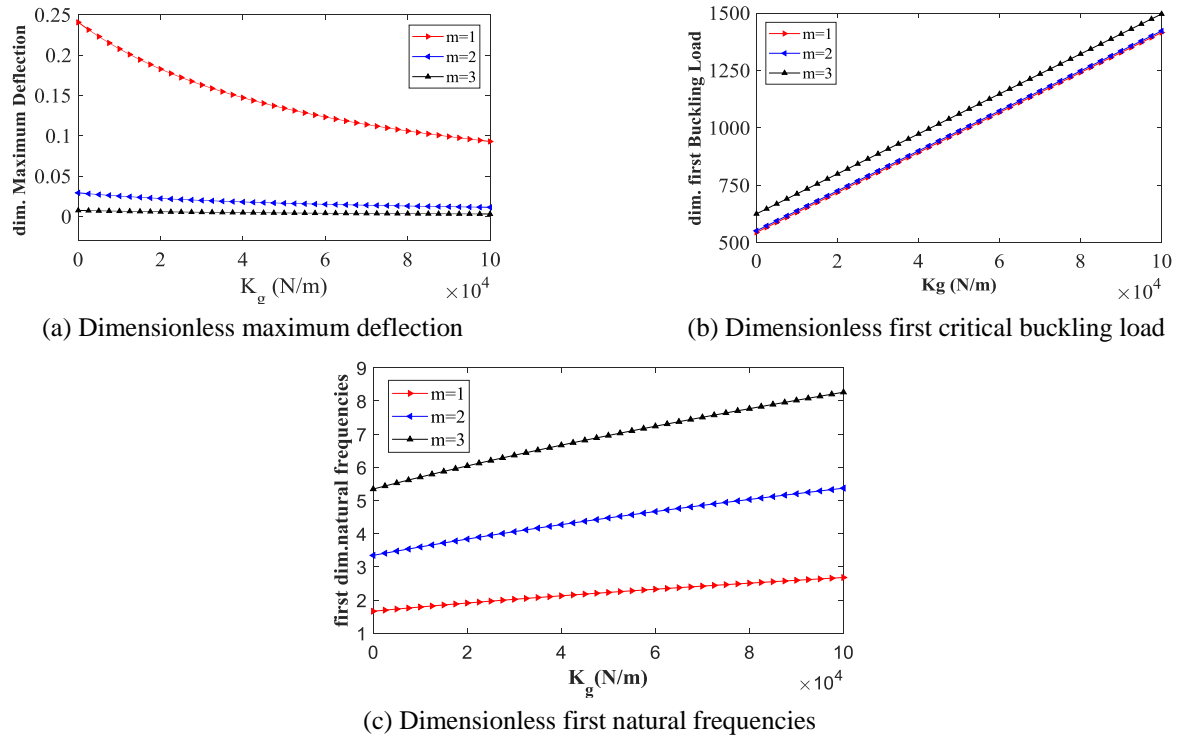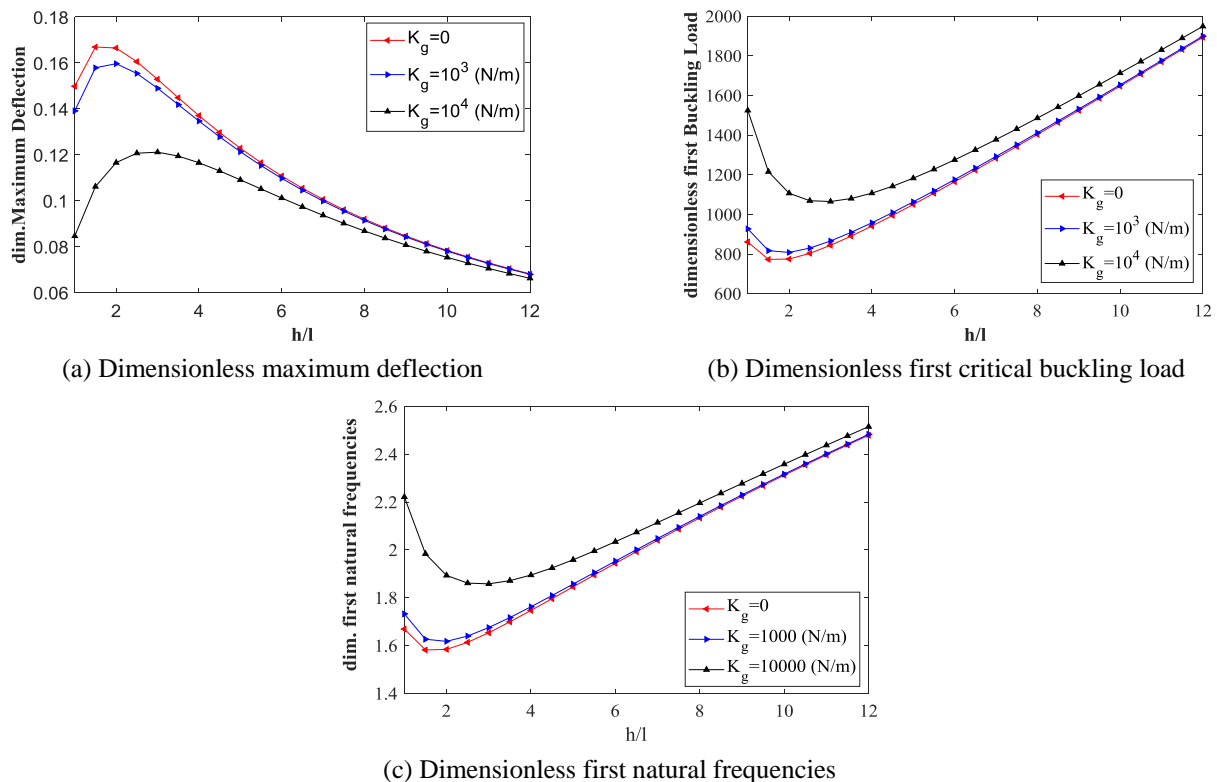
Fig. 8 depicts the effect of Pasternak shear moduli on

(a) Dimensionless maximum deflection

(b) Dimensionless first critical buckling load

(c) Dimensionless first natural frequencies

Fig. 8 Effects of Pasternak shear moduli versus axial wave numbers (m)

(a) Dimensionless maximum deflection

(b) Dimensionless first critical buckling load

(c) Dimensionless first natural frequencies

Fig. 9 Effects of thickness-to-length scale parameter versus various Pasternak shear moduli

the dimensionless maximum deflection, critical buckling load and free vibration behaviors of sinusoidal micro composite beam reinforced by SWCNTs for first three axial wave numbers. In the present study, the Navier's solution type is used to calculate natural frequencies, critical buckling load and maximum deflection of micro beam and m introduces as wave number that it shows mode numbers. As it is seen in this figure increasing mode number leads to increase the dimensionless natural frequencies and critical buckling load while reduces dimensionless maximum

deflection. Also, it is depicted that due to use the Pasternak shear moduli enhances the micro structure stiffness and these increasing have a special role on static and dynamic responses of micro composite beam. So that, the effect of Pasternak shear moduli is the same in various mode numbers and leads to increase stiffness of micro structure.

Fig. 9 considers the effect of Pasternak shear moduli on the dimensionless maximum deflection, critical buckling load and free vibration behaviors of sinusoidal micro composite beam reinforced by SWCNTs versus thickness-to-length scale parameter based on MSGT. As it is said that in the Fig. 3, the effect of material length scale parameters is noticeable for lower values of thickness-to-material length scale parameters. But, in this figure the effect of elastic foundation is considered and it is showed that the static and dynamic behaviors of microbeam are different for the various value of thickness-to-length scale parameter in presence of Pasternak shear moduli and Winkler spring constant. So that, the first dimensionless buckling load and natural frequencies decrease for $\frac{h}{l} < 3$ while these parameters increase for $\frac{h}{l} > 3$. Moreover, when the thickness-to-length scale parameter is small $\left(\frac{h}{l} < 3\right)$ the dimensionless maximum deflection enhances while this parameter is decreases with increasing the thickness-to-length scale parameter.

8. Conclusions

In this article, bending, buckling and free vibration analysis of a micro composite sinusoidal beam reinforced by single-walled carbon nanotubes embedded in an elastic medium in the presence of magnetic field under transverse uniform load with considering surface stress effect based on modified strain gradient theory is investigated. The governing equations of motion are obtained by Hamilton's principle and the Navier's type solution is used for simply supported boundary conditions. The generalized rule mixture is employed to predict temperature-dependent mechanical and thermal properties of micro composite beam. The influences of the material length scale parameters, elastic foundation, composite fiber angle, magnetic intensity, temperature changes and carbon nanotubes volume fraction on the bending, buckling and free vibration behaviors of micro beam are studied. The results of this research can be listed as follows:

(1) There is a small different between the presence and absence of the surface layer stress. The considering surface layer stress leads to decrease dimensionless maximum deflection and vice versa for buckling and vibration behaviors.

(2) The effect of surface Lame constant is more important than residual stresses, surface mass density and surface layer thickness. Moreover, the dimensionless critical buckling load and natural frequency increase with an increase in surface Lame constant while the dimensionless maximum deflection decreases.

(3) The material length scale parameter has greater effect on the static, buckling and free vibration behaviors of micro composite sinusoidal beam reinforced by SWCNTs. This effect leads to increase the stiffness of micro structure and it is more important for lower thickness-to-material length scale parameters of micro beam.

(4) The influence of the Pasternak shear modulus is more than the Winkler spring constant on the static, buckling and free vibration of micro composite beam. Anyway, with increasing both them, the dimensionless critical buckling load and natural frequency of micro beam increase while the dimensionless maximum deflection decreases.

(5) The magnetic field increases the stiffness of micro composite sinusoidal beam. This increasing stiffness is related to the intensity of magnetic field. The dimensionless critical buckling load and natural frequency increase by increasing the intensity magnetic field while the dimensionless maximum deflection decreases. Moreover, the effect of this parameter is more on the static response of micro beam.

(6) The carbon nanotube volume fraction leads to enhance the stiffness of micro composite structures.

(7) With increasing of temperature changes, the critical buckling load and natural frequency of micro composite sinusoidal beam decrease while the maximum deflection increases. Also, the influence of temperature changes on the structural behavior is less important compared to the other parameters.

(8) It is depicted that due to use the Pasternak shear moduli enhances the micro structure stiffness and these increasing have a special role on static and dynamic responses of micro composite beam. So that, the effect of Pasternak shear moduli is the same in various mode numbers and leads to increase stiffness of micro structure.

(9) It is showed that the static and dynamic behaviors of microbeam are different for the various value of thickness-to-length scale parameter in presence of Pasternak shear moduli and Winkler spring constant. So that, the first dimensionless buckling load and natural frequencies decrease for $\frac{h}{l} < 3$ while the maximum deflection increases for $\frac{h}{l} > 3$. Moreover, when the thickness-to-length scale parameter is small $\left(\frac{h}{l} < 3\right)$ the dimensionless maximum deflection enhances while this parameter decreases with increasing the thickness-to-length scale parameter.

References

Afshin, M. and Taheri, F. (2015), "Interlaminar stresses of laminated composite beams resting on elastic foundation subjected to transverse loading", *Comput. Materials. Sci.*, **96**, 439-447.

Aifantis, E.C. (1999), "Gradient deformation models at nano, micro and macro scales", *J. Eng. Mater. Technol.*, **121**(2), 189-202.

Akgöz, B. and Civalek, Ö. (2012), "Analysis of micro-sized beams for various boundary conditions based on the strain gradient elasticity theory", *Arch. Appl. Mech.*, **82**(3), 423-443.

Akgöz, B. and Civalek, Ö. (2014a), "A new trigonometric beam model for buckling of strain gradient microbeams", *Int. J. Eng. Sci.*, **81**, 88-94.

Akgöz, B. and Civalek, Ö. (2014b), "Thermo-mechanical buckling behavior of functionally graded microbeams embedded in elastic medium", *Int. J. Eng. Sci.*, **85**, 90-104.

Akgöz, B. and Civalek, Ö. (2015a), "A microstructure-dependent sinusoidal plate model based on the strain gradient elasticity theory", *Acta. Mech.*, **226**(7), 2277-2294.

Akgöz, B. and Civalek, Ö. (2015b), "Bending analysis of FG microbeams resting on Winkler elastic foundation via strain gradient elasticity", *Compos. Struct.*, **134**, 294-301.

Akgöz, B. and Civalek, Ö. (2016), "Bending analysis of embedded carbon nanotubes resting on an elastic foundation using strain gradient elasticity", *Acta Astronautica*, **119**, 1-12.

Ansari, R. and Sahmani, S. (2011), "Surface stress effects on the free vibration behavior of nanoplates", *Int. J. Eng. Sci.*, **49**(11), 1204-1215.

Ansari, R., Gholami, R. and Sahmani, S. (2011), "Free vibration analysis of size-dependent functionally graded microbeams based on the strain gradient Timoshenko beam theory", *Compos. Struct.*, **94**(1), 221-228.

Attia, M.A. and Mahmoud, F.F. (2016), "Modelling and analysis of nanobeams based on nonlocal-couple stress elasticity and surface energy theories", *Int. J. Mech. Sci.*, **105**, 126-134.

Civalek, Ö., Demir, C. and Akgöz, B. (2009), "Static analysis of single walled carbon nanotubes (SWCNT) based on Eringen's nonlocal elasticity theory", *Int. J. Engin. Appl. Sci.*, **1**(2), 47-56.

Ebrahimi, F. and Barati, M.R. (2016a), "Thermal buckling analysis of size-dependent FG nanobeams based on the third-order shear deformation beam theory", *Acta. Mech. Solid. Sinica*, **29**(5), 547-554.

Ebrahimi, F. and Barati, M.R. (2016b), "A nonlocal higher-order refined magneto-electro-viscoelastic beam model for dynamic analysis of smart nanostructures", *Int. J. Eng. Sci.*, **107**, 183-196.

Dai, H.L., Zhao, D.M., Zou, J.J. and Wang, L. (2016), "Surface effect on the nonlinear forced vibration of cantilevered nanobeams", *Phys. E.*, **80**, 25-30.

Eringen, A.C. (1967), "Theory of micropolar plates", *Z. Angew. Math. Phys.*, **18**, 12-30.

Eringen, A.C. (1972), "Nonlocal polar elastic continua", *Int. J. Eng. Sci.*, **10**(1), 1-16.

Fleck, N.A. and Hutchinson, J.W. (1993), "A phenomenological theory for strain gradient effects in plasticity", *J. Mech. Phys. Solids.*, **41**(12), 1825-1857.

Fleck, N.A. and Hutchinson, J.W. (2001), "A reformulation of strain gradient plasticity", *J. Mech. Phys. Solids.*, **49**(10), 2245-2271.

Ghorbanpour Arani, A. and Roudbari, M.A. (2014), "Surface stress, initial stress and Knudsen-dependent flow velocity effects on electro-thermo nonlocal wave propagation of SWBNNTs", *Phys. B.*, **452**, 159-165.

Jahangiri, R., Jahangiri, H. and Khezerloo, H. (2015), "FGM micro-gripper under electrostatic and intermolecular Van-der

Waals forces using modified couple stress theory", *Steel Compos. Struct., Int. J.*, **18**(6), 1541-1555.

Khorshidi, M.A., Shaat, M., Abdelkefi, A. and Shariati, M. (2017), "Nonlocal modeling and buckling features of cracked nanobeams with Von Karmen nonlinearity", *Appl. Phys. A*, **123**(1), 62-73.

Koiter, W.T. (1964), "Couple stresses in the theory of elasticity: I and II", *Proc. K. Ned. Akad. Wet. (B)*, **67**, 17-44.

Lam, D.C.C., Yang, F., Chong, A.C.M., Wang, J. and Tong, P. (2003), "Experiments and theory in strain gradient elasticity", *J. Mech. Phys. Solids*, **51**(8), 1477-1508

Lei, J., He, Y., Zhang, B., Gan, Zh. and Zeng, P. (2013a), "Bending and vibration of functionally graded sinusoidal microbeams based on the strain gradient elasticity theory", *Int. J. Eng. Sci.*, **72**, 36-52.

Lei, Z.X., Liew, K.M. and Yu, J.L. (2013b), "Buckling analysis of functionally graded carbon nanotube-reinforced composite plates using the element-free kp-Ritz method", *Compos. Struct.*, **98**, 160-168.

Lei, Z.X., Liew, K.M. and Yu, J.L. (2013c), "Free vibration analysis of functionally graded carbon nanotube-reinforced composite plates using the element-free kp-Ritz method in thermal environment", *Compos. Struct.*, **106**, 128-138.

Lei, Z.X., Zhang, L.W. and Liew, K.M. (2015), "Elastodynamic analysis of carbon nanotube-reinforced functionally graded plates", *Int. J. Mech. Sci.*, **99**, 208-217.

Li, Y.S. and Pan, E. (2015), "Static bending and free vibration of a functionally graded piezoelectric microplate based on the modified-stress theory", *Int. J. Eng. Sci.*, **97**, 40-59.

Lu, C.F., Chen, W.Q. and Lim, C.W. (2009a), "Elastic mechanical behavior of nano-scaled FGM films incorporating surface energies", *Compos. Sci. Technol.*, **69**(7-8), 1124-1130.

Lu, C.F., Lim, C.W. and Chen, W.Q. (2009b), "Size-dependent elastic behavior of FGM ultra-thin films based on generalized refined theory", *Int. J. Solid. Struct.*, **46**(5), 1176-1185.

Ma, H.M., Gao, X.L. and Reddy, J.N. (2008), "A microstructure-dependent Timoshenko beam model based on a modified couple stress theory", *J. Mech. Phys. Solids.*, **56**(12), 3379-3391.

McFarland, A.W. and Colton, J.S. (2005), "Role of material microstructure in plate stiffness with relevance to microcantilever sensors", *J. Micromech. Microeng.*, **15**(5), 1060-1067.

Mohammadi, H. and Mahzoon, M. (2013), "Thermal effects on postbuckling of nonlinear microbeams based on the modified strain gradient theory", *Compos. Struct.*, **106**, 764-776.

Mohammadimehr, M. and Mehrabi, M. (2017), "Stability and free vibration analysis of double-bonded micro composite sandwich cylindrical shells conveying fluid flow", *Appl. Math. Model.*, **47**, 685-709.

Mohammadimehr, M., Rousta Navi, B. and Ghorbanpour Arani, A. (2014), "Surface stress effect on the nonlocal biaxial buckling and bending analysis of polymeric piezoelectric nanoplate reinforced by CNT using Eshelby-Mori-Tanaka approach", *J. Solid. Mech.*, **7**(2), 173-190.

Mohammadimehr, M., Rousta Navi, B. and Ghorbanpour Arani, A. (2015), "Free vibration of viscoelastic double-bonded polymeric nanocomositr plates reinforced by FG-SWCNTs using MSGT, sinusoidal shear deformation theory and meshless method", *Compos. Struct.*, **131**, 654-671.

Mohammadimehr, M., Mohammadimehr, M.A. and Dashti, P. (2016a), "Size-dependent effect on biaxial and shear nonlinear buckling analysis of nonlocal isotropic and orthotropic micro-plate based on surface stress and modified couple stress theories using differential quadrature method", *Appl. Math. Mech.*, **37**(4), 529-554.

Mohammadimehr, M., Salemi, M. and Rousta Navi, B. (2016b), "Bending, buckling, and free vibration analysis of MSGT

microcomposite Reddy plate reinforced by FG-SWCNTs with temprature-dependent material properties under hydro-thermo-mechanical loadings using DQM", *Compos. Struct.*, **138**, 361-380.

Poole, W.J., Ashby, M.F. and Fleck, N.A. (1996), "Micro-hardness of annealed and work-hardened copper polycrystals", *Scr. Mater.*, **34**(4), 559-564

Shaat, M. (2015b), "Effects of grain size and microstructure rigid rotations on the bending behavior of nanocrystalline material beams", *Int. J. Mech. Sci.*, **94-95**, 27-35.

Shaat, M. and Abdelkefi, A. (2015a), "Pull-in instability of multi-phase nanocrystalline silicon beams under distributed electrostatic force", *Int. J. Mech. Sci.*, **90**, 58-75.

Shaat, M. and Abdelkefi, A. (2017), "Material structure and size effects on the nonlinear dynamics of electrostatically-actuated nano-beams", *Int. J. Nonlin. Mech.*, **89**, 25-42.

Shaat, M., Mahmoud, F.F., Alshorbagi, A.E., Alieldin, S.S. and Meletis, E.I. (2012), "Size-dependent analysis of functionally graded ultra-thin films", *Struct. Eng. Mech., Int. J.*, **44**(4), 431-448.

Shaat, M., Eltaher, M.A., Gad, A.I. and Mahmoud, F.F. (2013), "Nonlinear size-dependent finite element analysis of functionally graded elastic tiny-bodies", *Int. J. Mech. Sci.*, **77**, 356-364.

Shen, H.S. (2009), "Nonlinear bending of functionally graded carbon nanotube-reinforced composite plates in thermal environments", *Compos. Struct.*, **91**(1), 9-19.

Simsek, M. and Reddy, J.N. (2013), "Bending and vibration of functionally graded microbeams using a new higher order beam theory and the modified couple stress theory", *Int. J. Eng. Sci.*, **64**, 37-53.

Thai, H.T. and Vo, T.P. (2013a), "A new sinusoidal shear deformation theory for bending, buckling and vibration of functionally graded plates", *App. Math. Model.*, **37**(5), 3269-3281.

Thai, H.T. and Vo, T.P. (2013b), "A size-dependent functionally graded sinusoidal plate model based on a modified couple stress theory", *Compos. Struct.*, **96**, 376-383.

Yang, J. Xiong, J., Ma, L., Zhang, G., Wang, X. and Wu, L. (2014), "Study on vibration damping of composite sandwich cylindrical shell with pyramidal truss-like cores", *Compos. Struct.*, **117**, 362-372.

Zhu, P., Lei, Z.X. and Liew, K.M. (2012), "Static and free vibration analysis of carbon nanotube-reinforced composite plates using finite element method with first order shear deformation plate theory", *Compos. Struct.*, **94**(4), 1450-1460.

CC

Nomenclature

u, v, w	Displacement of micro beam in x, y and z directions, respectively
φ_x	Angle of rotation
SWCNT, SWBNNT	Single walled Carbon nanotube and boron nitride nanotube, respectively
MEMS, NEMS	Micro electro mechanical system and Nano electro mechanical system, respectively
FSDT, TSDT, SSDT	First order, Third-order and sinusoidal shear deformation theories, respectively
MCST	Modified couple stress theory
MSGT	Modified strain gradient theory
FGM	Functionally graded material
$w_{CNT}, \rho_{CNT}, V_{CNT}$	Mass fraction, density and volume fraction of carbon nanotubes, respectively
E_{11}^{CNT}, E_{11}^{CNT}, G_{12}^{CNT}	Young's and shear modulus of carbon nanotube, respectively
ρ^m, V^m	density and volume fraction of matrix, respectively
E_m, G_m	Young's and shear modulus of matrix, respectively
η_i	Force transformation between carbon nanotubes and matrix
ε_{ij}, γ_i, $\eta_{ijk}^{(1)}$, $\chi_{ij}^{(s)}$	Classical strain, dilatation gradient, deviatoric stretch gradient and symmetric rotation gradient tensors, respectively
σ_{ij}, p_i, $\tau_{ijk}^{(1)}$, $m_{ij}^{(s)}$	Components of classical and higher order stresses tensors, respectively
α_{11}	Thermal expansion coefficient
C_{11}, C_{55}	Transformation reduced plane stiffness and transformation transverse shear stiffness, respectively
θ	Composite fiber angle
l_0, l_1, l_2	Additional length scale parameters
τ^s, E^s, ρ^s	Residual stresses, Lame constant and surface mass density, respectively
H, h, J, η	Magnetic intensity vector, perturbation magnetic field, electriccurrent density vector and magnetic permeability, respectively
f_l	Lorentz forces
K_s	Shear correction factor
t	Thickness of surface layer
T, U, U^s	Kinetic, total potential strain, surface stress energy
$V^{elastic}, V^{fl}, V$	Work done by external work
U_m, W_m, φ_m	Undetermined Fourier coefficient
ω	Vibration frequency

Appendix A

The obtained results from Eq. (11) are presented in this appendix that they can be written as follows

$$\varepsilon_x = \frac{\partial u_0(x,t)}{\partial x} - z\frac{\partial^2 w_0(x,t)}{\partial x^2} + R(z)\frac{\partial \phi_X(x,t)}{\partial x} \quad \text{(A1)}$$

$$\varepsilon_{xz} = \frac{1}{2}\frac{\partial R(z)}{\partial z}\phi_X(x,t) \quad \text{(A2)}$$

$$\gamma_x = \frac{\partial^2 u_0}{\partial x^2} - z\frac{\partial^3 w_0}{\partial x^3} + R\frac{\partial^2 \phi}{\partial x^2} \quad \text{(A3)}$$

$$\gamma_z = -\frac{\partial^2 w_0}{\partial x^2} + \frac{\partial R}{\partial z}\frac{\partial \phi}{\partial x} \quad \text{(A4)}$$

$$\eta_{xxx}^{(1)} = \frac{2}{5}[\frac{\partial^2 u_0}{\partial x^2} - z\frac{\partial^3 w_0}{\partial x^3} + R\frac{\partial^2 \phi}{\partial x^2} - \frac{1}{2}\frac{\partial^2 R}{\partial z^2}\phi] \quad \text{(A5)}$$

$$\eta_{xxz}^{(1)} = \eta_{xzx}^{(1)} = \eta_{zxx}^{(1)} = \frac{4}{15}\left[-\frac{\partial^2 w_0}{\partial x^2} + 2\frac{\partial R}{\partial z}\frac{\partial \phi}{\partial x}\right] \quad \text{(A6)}$$

$$\eta_{xyy}^{(1)} = \eta_{yxy}^{(1)} = \eta_{yyx}^{(1)} = -\frac{1}{5}\left[\frac{\partial^2 u_0}{\partial x^2} - z\frac{\partial^3 w_0}{\partial x^3} + R\frac{\partial^2 \phi}{\partial x^2} + \frac{1}{3}\frac{\partial^2 R}{\partial z^2}\phi\right] \text{(A7)}$$

$$\eta_{xzz}^{(1)} = \eta_{zxz}^{(1)} = \eta_{zzx}^{(1)} = -\frac{1}{5}\left[\frac{\partial^2 u_0}{\partial x^2} - z\frac{\partial^3 w_0}{\partial x^3} + R\frac{\partial^2 \phi}{\partial x^2} - \frac{4}{3}\frac{\partial^2 R}{\partial z^2}\phi\right] \text{(A8)}$$

$$\eta_{yyz}^{(1)} = \eta_{yzy}^{(1)} = \eta_{zyy}^{(1)} = -\frac{1}{15}\left[-\frac{\partial^2 w_0}{\partial x^2} + 2\frac{\partial R}{\partial z}\frac{\partial \phi}{\partial x}\right] \quad \text{(A9)}$$

$$\eta_{zzz}^{(1)} = \frac{1}{5}\left[\frac{\partial^2 w_0}{\partial x^2} - 2\frac{\partial R}{\partial z}\frac{\partial \phi}{\partial x})\right] \quad \text{(A10)}$$

$$\chi_{yx}^{(s)} = \chi_{xy}^{(s)} = -\frac{1}{2}\left[\frac{\partial^2 w_0}{\partial x^2} - \frac{1}{2}\frac{\partial R}{\partial z}\frac{\partial \phi}{\partial x}\right] \quad \text{(A11)}$$

$$\chi_{yx}^{(s)} = \chi_{xy}^{(s)} = -\frac{1}{2}\left[\frac{\partial^2 w_0}{\partial x^2} - \frac{1}{2}\frac{\partial R}{\partial z}\frac{\partial \phi}{\partial x}\right] \quad \text{(A12)}$$

Appendix B

Components of stiffness, mass, buckling and external force matrices are showed in this appendix that they can be written as follows

$$k_{11} = \beta^2\left[A_{11} + A_0^s + A_1^s - Y^{(1)} + (P^{(0)} + \frac{5}{2}T^{(0)})\beta^2\right] \quad \text{(B1)}$$

$$k_{12} = -\beta^3\left[B_{11} + B_0^s + B_1^s - \tau^s q_z^{(1)} + (P^{(1)} + \frac{5}{2}T^{(1)})\beta^2\right] \text{(B2)}$$

$$k_{13} = Y^{(5)} + (B_{11}^{'} + B_0^{'s} + B_1^{'s} + \frac{5}{4}T^{(1)} - Y^{(3)})\beta^2 + (P^{(2)} + \frac{5}{2}T^{(3)})\beta^4 \text{(B3)}$$

$$k_{21} = -\beta^3\left[B_{11} + B_0^s + B_1^s + (P^{(1)} + \frac{5}{2}T^{(1)})\beta^2\right] \quad \text{(B4)}$$

$$k_{22} = k_w + (k_g - Y^{(3)})\beta^2 + (D_{11} + D_0^s + D_1^s + -\tau^s q_z^{(2)}$$
$$+ P^{(0)} + \frac{5}{3}T^{(0)} + M^{(0)} - Y^{(2)})\beta^4 + (P^{(3)} + \frac{5}{2}T^{(4)})\beta^6 \quad \text{(B5)}$$

$$k_{23} = -\beta\left[\begin{array}{l}Y^{(6)} + (B_{11}^{'} + D_0^{'s} + D_1^{'s} + P^{(6)} + \frac{5}{4}T^{(6)} + \frac{8}{3}T^{(0)} + \frac{2}{3}T^{(10)} \\ +\frac{1}{2}M^{(1)} - Y^{(4)})\beta^2 + (P^{(4)} + \frac{5}{2}T^{(5)})\beta^4\end{array}\right] \text{(B6)}$$

$$k_{31} = \beta^2\left[B_{11}^{'} + B_0^{'s} + B_1^{'s} + \frac{5}{4}T^{(3)} - Y^{(3)} + (P^{(2)} + \frac{5}{2}T^{(2)})\beta^2\right] \text{(B7)}$$

$$k_{32} = -\beta\left[\begin{array}{l}-B_2^s - B_3^s + (B_{11}^{'} + D_0^{'s} + D_1^{'s} - \tau^s q_z^{(3)} + P^{(7)} + \frac{5}{4}T^{(6)} - \frac{10}{3}T^{(10)} \\ -\frac{1}{2}M^{(1)} + Y^{(4)})\beta^2 + (P^{(4)} + \frac{5}{2}T^{(5)})\beta^4\end{array}\right] \text{(B8)}$$

$$k_{33} = (D_{55}^R + \frac{5}{3}T^{(9)} + \frac{1}{4}M^{(3)} + Y^{(7)}) + (B_{11}^R + R_0^s + R_1^s + P^{(8)} + \frac{5}{2}T^{(8)}$$
$$+ \frac{20}{3}T^{(11)} + \frac{1}{4}M^{(2)} - Y^{(3)})\beta^2 + (P^{(5)} + \frac{5}{2}T^{(7)})\beta^4 \quad \text{(B9)}$$

$$M_{11} = I^{(0)} \quad \text{(B10)}$$

$$M_{12} = (\rho^s q_z^{(1)} - I^{(1)})\beta \quad \text{(B11)}$$

$$M_{13} = I^{(3)} \quad \text{(B12)}$$

$$M_{21} = -I^{(1)}\beta \quad \text{(B13)}$$

$$M_{22} = (I^{(2)} - \rho^s q_z^{(2)})\beta^2 + I^{(0)} \quad \text{(B14)}$$

$$M_{23} = -I^{(4)}\beta \quad \text{(B15)}$$

$$M_{31} = I^{(3)} \quad \text{(B16)}$$

$$M_{32} = (\rho^s q_z^{(3)} - I^{(4)})\beta \quad \text{(B17)}$$

$$M_{33} = I^{(5)} \quad \text{(B18)}$$

$$\begin{cases} N_{11} = N_{12} = N_{13} = 0 \\ N_{21} = N_{23} = 0 \\ N_{31} = N_{32} = N_{33} = 0 \end{cases} \tag{B19}$$

$$N_{22} = \beta^2 \tag{B20}$$

$$f_1 = -\frac{4\alpha_{11}\Delta T}{L}(hC_{11} + 2tE^s) \tag{B21}$$

$$f_2 = \frac{4q_0}{n\pi} \tag{B22}$$

$$f_3 = 0 \tag{B23}$$

Where in the above equations, the value of β are considered equal to $\frac{m\pi}{L}$.